Supplementary Information

Plant-like biosynthesis of isoquinoline alkaloids in *Aspergillus fumigatus*

Joshua A. Baccile[1,#], Joseph E. Spraker[2,#], Henry H. Le[1], Eileen Brandenburger[3], Christian Gomez[1], Jin Woo Bok[4], Juliane Macheleidt[5], Axel A. Brakhage[5], Dirk Hoffmeister[3], Nancy P. Keller[4,6]*, Frank C. Schroeder[1,*]

[1]Boyce Thompson Institute and Department of Chemistry and Chemical Biology, Cornell University, Ithaca, NY, United States

[2]Department of Plant Pathology, University of Wisconsin-Madison, WI, United States

[3]Department of Pharmaceutical Microbiology at the Hans-Knöll-Institute, Friedrich Schiller University, Jena, Germany

[4]Department of Bacteriology, University of Wisconsin-Madison, WI, United States

[5]Molecular and Applied Microbiology, Leibniz Institute for Natural Product Research and Infection Biology (HKI), and Institute for Microbiology, Friedrich Schiller University, Jena, Germany

[6]Department of Medical Microbiology and Immunology, University of Wisconsin-Madison, WI, United States

[#]These authors contributed equally
*To whom correspondence should be directed

Supplementary Results

Supplemetary Table 1. LC-HRMS data of reported compounds

Compound	HR-ESI(+/-) observed (*m/z*)	Ion	Calculated ion formula	Calculated *m/z*	Retention time [min]	Yield of compound (per L culture)*
1	281.1137	$[M+H]^+$	$C_{13}H_{17}N_2O_5^+$	281.1132	0.74	~1–5 mg
2	359.0557	$[M-H]^-$	$C_{13}H_{15}N_2O_8S^-$	359.0555	0.81	~1–5 mg
3	289.0471	$[M-H]^-$	$C_{13}H_9N_2O_6^-$	289.0466	4.31	~10–50 mg
4	241.0255	$[M-H]^-$	$C_{12}H_5N_2O_4^-$	241.0255	4.38	
5	227.0462	$[M-H]^-$	$C_{12}H_7N_2O_3^-$	227.0462	6.58	
7	200.0727	$[M-H]^-$	$C_{12}H_{10}NO_2^-$	200.0717	7.46	~0.5–2 mg
8	216.0676	$[M-H]^-$	$C_{12}H_{10}NO_3^-$	216.0666	5.98	~0.5–2 mg
11	210.0772	$[M-H]^-$	$C_{10}H_{12}NO_4^-$	210.0772	1.71	
12	208.0615	$[M-H]^-$	$C_{10}H_{10}NO_4^-$	208.0165	1.38	
18	293.0565	$[M-H]^-$	$C_{16}H_9N_2O_4^-$	293.0568	5.46	~1–5 mg
21	343.0941	$[M-H]^-$	$C_{17}H_{15}N_2O_6^-$	343.0936	4.31	
22	337.0473	$[M-H]^-$	$C_{17}H_9N_2O_6^-$	337.0466	5.13	

*Numbers indicate estimated production of each compound prior to sample treatment, where significant losses are incurred at each chromatographic step.

Supplementary Table 2. Predicted homologs of *fsqB*, *fsqC*, and *fsqG* that are clustered in other *Aspergilli*.

Protein	Identity* (%) to genes of				Putative function
A. fumigatus 293	*N. fischeri*	*A. parasiticus*	*A. oryzae*	*A. flavus*	
fsqB	474/497 (95%)	234/501 (47%)	232/501 (46%)	228/501 (46%)	FAD binding domain protein
fsqC	338/365 (93%)	157/321 (49%)	160/343 (47%)	158/325 (49%)	methyltransferase
fsqG	557/598 (93%)	329/619 (53%)	326/619 (53%)	330/619 (53%)	cytochrome P450 monooxygenase

*Percentage similarity values of the *A. fumigatus* 293 ORFs to *N. fischeri, A. parasiticus, A. oryzae,* and *A. flavus* clusters are given in parentheses.

Supplementary Table 3. Amino acid sequence of polyhistidine-tagged FsqB and software-aided[1] identification of tryptic FsqB peptides analyzed with UHPLC-MS/MS.

MGSSHHHHHHSSGLVPRGSHMSIPNSFIIVGSGVFGLSLAYALSLDDRFADKKIILVDRWNFEPPNATGSVHNPAAAN
ADTSRVIRRDYPHGPYASLALEAMKHWRGKFGENNRYVNQRLLFSGEGSSLTTPPKALETVNYIKKAYAISCELTPGG
RDAVQVLDSLDEVRAFLGNTPSHPPHLPVNKDPAARDLRGYVSNDCGWADAGASIEWLRQEVLRLGRVECVVGEVE
SLVYSDDQRAVKGVKLVDGKVLTAELTVIAAGARSSHILGIPKLCDVYSEFVAYIQLTKEEADELRRRQWPILVNCHRG
VFAVGPDHDNCLKFGHFSYSGIVDVLREASIQVPTRPDGWEAQQKYWSDPRFAFGGEVKVSALGDVDDYENPAAQR
ALADYRLFLLELLGPTGLQGVDTLGLDQSDNLLNNIANRPFTRVRKCWYNDTPALDFVVDYHPSYGKTLFVATGGCD
HAFKFLPIIGEKTLALILRNRGDSAVSLPAGVEPSLEELSELWRFPVELLQDN

Peptide	observed	expected	z	Δ
MGSSHHHHHHSSGLVPR	590.2879	633.9679	3	-131.0400
GSHMSIPNSFIIVGSGVFGLSLAYALSLDDRFADKKIILVDR	1075.2218	1075.2200	3	0.0254
WNFEPPNATGSVHNPAAANADTSR	842.0560	842.0509	3	-0.0066
DYPHGPYASLALEAMK	881.9266	881.9198	2	-0.0010
FGENNR	736.3424	736.3373	1	0.0051
LLFSGEGSSLTTPPK	767.4106	767.4043	2	-0.0020
ALETVNYIK	1050.5813	1050.5757	1	-0.0017
AYAISCELTPGGR	697.8393	697.8330	2	-0.0020
DAVQVLDSLDEVR	1458.7411	1458.7362	1	-0.0024
FLGNTPSHPPHLPVNK	457.2478	457.2409	4	-0.0015
GYVSNDCGWADAGASIEWLR	1113.9964	1113.9900	2	-0.0018
VECVVGEVESLVYSDDQR	1041.9851	1041.9788	2	-0.0020
VLTAELTVIAAGAR	462.2763	462.2695	3	-0.0014
SSHILGIPK	951.5615	951.5549	1	-0.0007
LCDVYSEFVAYIQLTK	974.9887	974.9826	2	-0.0023
EEADELR	431.2024	431.1938	2	0.0027
QWPILVNCHR	661.8428	661.8357	2	-0.0003
GVFAVGPDHDNCLK	764.8631	764.8570	2	-0.0024
FGHFSYSGIVDVLR	798.9108	798.9048	2	-0.0026

EASIQVPTRPDGWEAQQK	1020.5093	1020.5036	2	-0.0032
YWSDPR	412.1909	412.1903	2	0.0012
FAFGGEVK	854.4397	854.4334	1	-0.0009
VSALGDVDDYENPAAQR	910.4254	910.4192	2	-0.0022
LFLLELLGPTGLQGVDTLGLDQSDNLLNNIANRPFTR	1346.7254	1346.7195	3	-0.0042
KCWYNDTPALDFVVDYHPSYGK	1134.4530	892.7407	3	725.1369
TLFVATGGCDHAFK	762.3686	762.3620	2	-0.0013
FLPIIGEK	916.5490	916.5429	1	-0.0012
TLALILR	799.5390	799.5327	1	-0.0009
GDSAVSLPAGVEPSLEELSELWR	1221.1133	1221.1061	2	-0.0002
FPVELLQDN	1074.5451	1074.5393	1	-0.0015
KC(FAD)WYNDTPALDFVVDYHPSYGK	1134.4530	1134.4454	3	0.0009

Supplementary Table 4. Fungal strains and plasmids used in this study

Strain/plasmid	Description	Reference
***Aspergillus fumigatus* 293 background strains**		
Af293	Wild type	2
Af293.1	*pyrG1*	2
Af293.6	*pyrG1, argB1*	2
TJES1.18	*A.fargB::gpdA(p):: fsqA, pyrG1*	This study
TJES2.20	*ΔfsqA::A.ppyrG, argB1*	This study
TJES3.1	*A.fargB::gpdA(p):: fsqA, A.ppyrG*	This study
TJES4.10	*A.fargB::gpdA(p):: fsqA, ΔfsqF::A.ppyrG*	This study
TJES8.2	*ΔfsqA::A.ppyrG, A.fargB*	This study
TJES13.61	*A.fargB::gpdA(p):: fsqA, ΔfsqB::A.ppyrG*	This study
TJES14.68	*A.fargB::gpdA(p):: fsqA, ΔfsqC::A.ppyrG*	This study
TJES15.91	*A.fargB::gpdA(p):: fsqA, ΔfsqG::A.ppyrG*	This study
***Aspergillus flavus* NRRL3357 background strains**		
NRRL3357.5	*pyrG1*	3
TJW149.27	*Δku70::pyrG*	This study
TJES19.1	*ΔpyrG, Δku70*	This study
TJES 23.3	*A.ppyrG::gpdA(p)::imqA, Δku70*	This study
TJES 27.1	*ΔimqA::A.ppyrG, Δku70*	This study
Plasmids		
pJMP4	*A. fumigatus argB*	4
pJMP8.1	*A. nidulans* gpdA promoter (truncated to 1.5 kb) in pBluescript	5
pJMP9.1	*A. nidulans gpdA(p) + A parasiticus pyrG*	6
pJES1.2	*gpdA(p):: fsqA* in *pJMP8.1*	This study
pJES2.7	*A. fumigatus argB::gpdA(p):: fsqA*	This study
pJES13.2	C-terminal 6His tagged *fsqF* A-domain in pET30a vector	This study
pJW24	*A parasiticus pyrG* in pBluescript	7

pXX = plasmid, TXX = original transformant

Supplementary Table 5. PCR primer sets used in this study

Name of the primer	Oligonucleotide sequence (5'-3')	Uses
Afu6g03380_FOR_Nprobe	CTTTCACGTGGACACTGCGC	Northern probe
Afu6g03380_REV_Nprobe	TACTGCTCCAACCAGCACCG	Northern probe
Afu6g03390_FOR_Nprobe	TCAGGGAGATATGGTGGCG	Northern probe
Afu6g03390_REV_Nprobe	CAACGCAGCAGGTAGTCACG	Northern probe
Afu6g03400_FOR_Nprobe	CTTCCAAGCCCAACAAGCC	Northern probe
Afu6g03400_REV_Nprobe	AATCTCGTAGGCCTCCAGCG	Northern probe
Afu6g03430_FOR_Nprobe	TGGCCTATCACACCAGTGGC	Northern probe
Afu6g03430_REV_Nprobe	GTGCAGCCTGAATCTCACGG	Northern probe
Afu6g03420_FOR_Nprobe	GAGCTCGACAATGGTGAGCG	Northern probe
Afu6g03420_REV_Nprobe	CAATCACATCGGCATGCGG	Northern probe
Afu6g03440_FOR_Nprobe	GATGGAACTTCGAGCCACCC	Northern probe
Afu6g03440_REV_Nprobe	GGCGATAATCTGCCAACGCC	Northern probe
Afu6g03450_FOR_Nprobe	CTACATCGCCTGCGATGTGG	Northern probe
Afu6g03450_REV_Nprobe	TAGCACACGCGCCAGATACC	Northern probe
Afu6g03460_FOR_Nprobe	GCGACTTCGCGACTCGGAAT	Northern probe
Afu6g03460_REV_Nprobe	CCATCACAAACTCGGTCCCG	Northern probe
Afu6g03470_FOR_Nprobe	AACTGCGCTCCAAAACCGCC	Northern probe
Afu6g03470_REV_Nprobe	ATCCACAAGGGCGATCTGGC	Northern probe
Afu6g03490_FOR_Nprobe	GTTCTCAGGGGATGTGACCG	Northern probe
Afu6g03490_REV_Nprobe	ACAAGTTCGCCCTTCGCTCCG	Northern probe
Afu6g03500_FOR_Nprobe	GGTGCTCAAGGAACAGAGGG	Northern probe
Afu6g03500_REV_Nprobe	GCCAAGAGGTCATTCTGCCC	Northern probe
Afu6g03510_FOR_Nprobe	AACACCCGATACCAGCTCGC	Northern probe
Afu6g03510_REV_Nprobe	ATGGGCCACCCATTGATGGC	Northern probe
Afu6g03520_FOR_Nprobe	ATGCCATCATCACCGGTGCC	Northern probe
Afu6g03520_REV_Nprobe	CGAGCATGGACAATAGCC	Northern probe
A.ppyrG_T7 FOR	CGTAATACGACTCACTATAGGG	Amplification of A.ppyrG from pJMP9.1
A.ppyrGR_Rev	ATTCGACAATCGGAGAGGCTGC	Amplification of A.ppyrG from pJMP9.1
Afu6g03430_3'F_flank	CTGTCGCTGCAGCCTCTCCGATTGTCG AATGCTTCAGCTGGAGTGTCTCC	Amplification of *fsqA* 3' flanking region
Afu6g03430_3'R_flank	TACAGCGACGACCAACGAGC	Amplification of *fsqA* 3' flanking region
Afu6g03430_5'F_flank	TAAGAGCGGAGACTGGTGGC	Amplification of *fsqA* 5' flanking region
Afu6g03430_5'R_flank	CCAATTCGCCCTATAGTGAGTCGTATT ACGTCTGCAAGGGTTTACGAGGG	Amplification of *fsqA* 5' flanking region
Afu6g03440_3'F_flank	CTGTCGCTGCAGCCTCTCCGATTGTCG AATTCGGAACTCTGGAGGTTCCC	Amplification of *fsqB* 3' flanking region
Afu6g03440_3'R_flank	ACTGCGCGACAAATGCAGCC	Amplification of *fsqB* 3' flanking region
Afu6g03440_5'F_flank	GTCTCGTCACTTACCCTGCC	Amplification of *fsqB* 5'

		flanking region
Afu6g03440_5'R_flank	CCAATTCGCCCTATAGTGAGTCGTATTACGAAAGAGACAGCCGGGATCCG	Amplification of *fsqB* 5' flanking region
Afu6g03450_3'F_flank	CTGTCGCTGCAGCCTCTCCGATTGTCGAATCTTGCTGCGGAAATCGAGCG	Amplification of *fsqC* 3' flanking region
Afu6g03450_3'R_flank	CACGGTAAAAGCCCAGTCCG	Amplification of *fsqC* 3' flanking region
Afu6g03450_5'F_flank	GATGTAGGCCACGAACTCGC	Amplification of *fsqC* 5' flanking region
Afu6g03450_5'R_flank	CCAATTCGCCCTATAGTGAGTCGTATTACGAGGATGCCAAAAGCCCACCG	Amplification of *fsqC* 5' flanking region
Afu6g03480_3'F_flank	CTGTCGCTGCAGCCTCTCCGATTGTCGAATCGCGGGCATCTAGTATTCGG	Amplification of *fsqF* 3' flanking region
Afu6g03480_3'R_flank	ACTTGCGCAACCAGCTGTGC	Amplification of *fsqF* 3' flanking region
Afu6g03480_5'F_flank	GAATCTGAGCGCTTGTCGCG	Amplification of *fsqF* 5' flanking region
Afu6g03480_5'R_flank	CCAATTCGCCCTATAGTGAGTCGTATTACGAAGAAAGGCGAAACGGAGCG	Amplification of *fsqF* 5' flanking region
Afu6g03490_3'F_flank	CTGTCGCTGCAGCCTCTCCGATTGTCGAATATGGACTCCAGTCAGGACCG	Amplification of *fsqG* 3' flanking region
Afu6g03490_3'R_flank	ATCCACCTCGTGGAGAAGCC	Amplification of *fsqG* 3' flanking region
Afu6g03490_5'F_flank	TGTGTCACGAAGGCAGTGCG	Amplification of *fsqG* 5' flanking region
Afu6g03490_5'R_flank	CCAATTCGCCCTATAGTGAGTCGTATTACGGTGCCCATCGTCCAATACGG	Amplification of *fsqG* 5' flanking region
fqsF_Adomain_xp_5'F	AATAA**GCGGCCGC**ACCTGGAACACCGTGGTTGC	Amplification of *fsqF* A-domain **(NotI cut site)**
fqsF_Adomain_xp_3' R	ATTAGC**CTCGAG**TTCGTTGCCCCGAGTGTGC	Amplification of *fsqF* A-domain **(XhoI cut site)**
fsqD_xp_5' F	GTAGGCTA**GAATTC**TCACACCAGCCTCTCTTGGC	Amplification of *fsqD* ORF **(EcoRI cut site)**
fsqD_xp_3' R	CATTAT**AAGCTT**GAGAAAGGAGTAGCGGACCTCTTCCC	Amplification of *fsqD* ORF **(HindIII cut site)**
Afu6g03430_NcoI_FOR	CAGATG**CCATGG**ACGACAAGCATGGCC	Amplification of *fsqA* ORF **(NcoI cut site)**
Afu6g03430_NotI_REV	GCAACC**GCGGCCGC**AGACAGCGCGGTATCACTG	Amplification of *fsqA* ORF **(NotI cut site)**
flvku70F5	ACATCTCTTCCGTCAAAGGCGC	Amplification of *ku70* 5’ flanking region
flavku70R5	CGATATCAAGCTATCGATACCTCGACTCTGTGTTGAGAGTCGTAAGTCATGAATTGCG	Amplification of *ku70* 5’ flanking region
flvku70F3	GTCGCTGCAGCCTCTCCGATTGTCGAATGACAACGCTAGTATTGGTTACGAGAG	Amplification of *ku70* 3’ flanking region

	ACAG	
flavku70R3	AGAATGGCTACGTCAACCTCCG	Amplification of *ku70* 3' flanking region
Fku70IF	ATGAGGAAGAGGAGGAGACCG	Amplification of Δ*ku70* cassette
Fku70IR	CACTTTTCAATCGTGCGAGCCG	Amplification of Δ*ku70* cassette
pet28_fsqB_3'_fwd	TGGTGCCGCGCGGCAGCCATATGTC TATCCCTAACTCTTTCATCATTGT	Amplification of fsqB, pET28b+ 3' destination
fsqB_5'_pet28_rev	CTCAGCTTCCTTTCGGGCTTTGTTACTA GTTGTCCTGTAGTAGTTCCACGG	Amplification of fsqB pET28b+ 5' destination

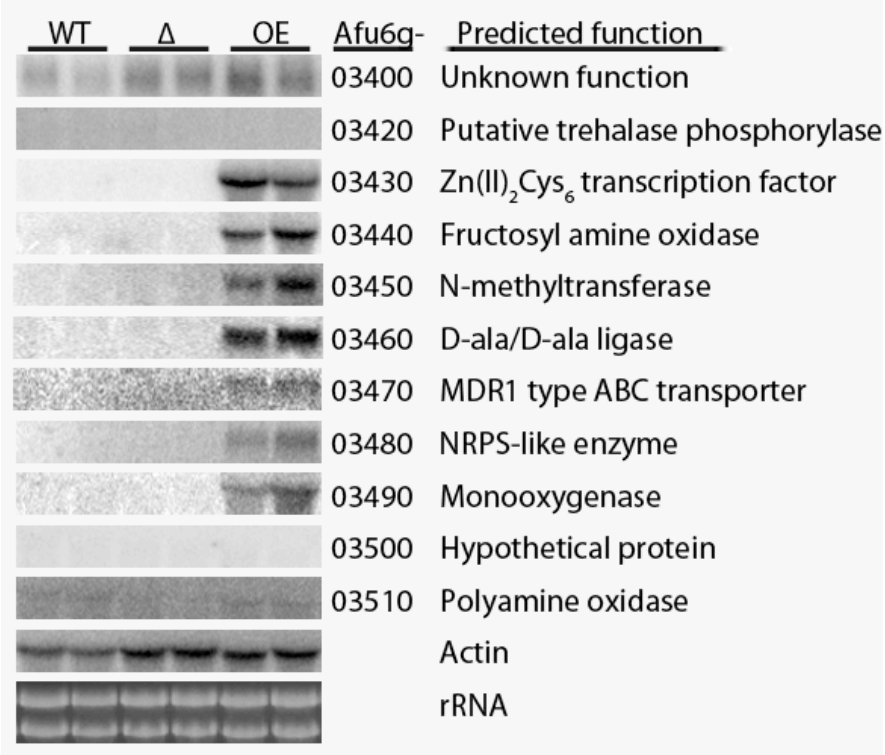

Supplementary Figure 1. Northern blot analysis of WT (Af293) left, Δ*fsqA* middle, and OE::*fsqA*, right. Overexpression of *fsqA* causes specific up-regulation of AFUA6g_03430 – AFUA6g_03490, defining the boundaries of the *fsq* cluster.

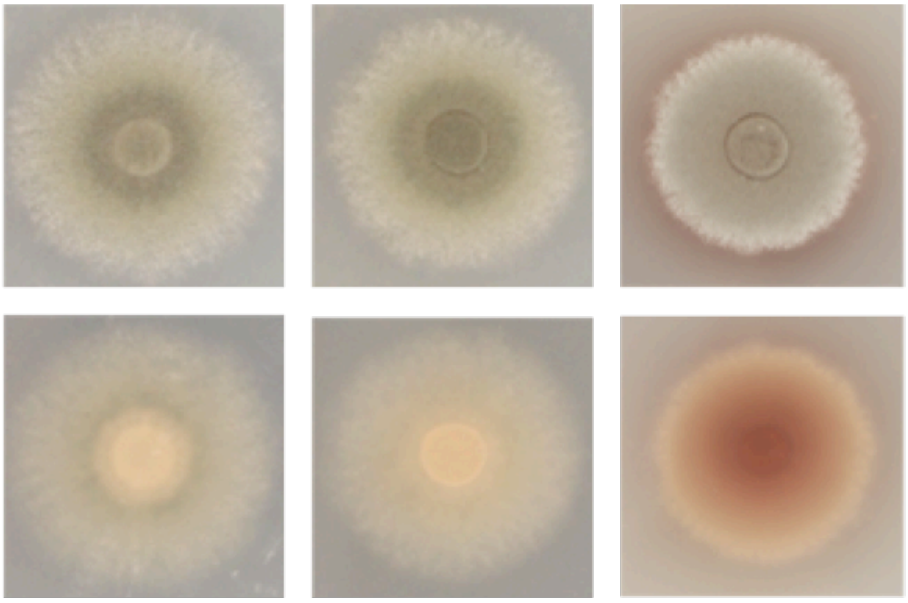

Supplementary Figure 2. Phenotype of WT (Af293) left, Δ*fsqA* middle, and OE::*fsqA* right grown on GMM at 37ºC for 72 hours. OE::*fsqA* decreases radial growth and shows characteristic brown pigmentation diffusing into the media.

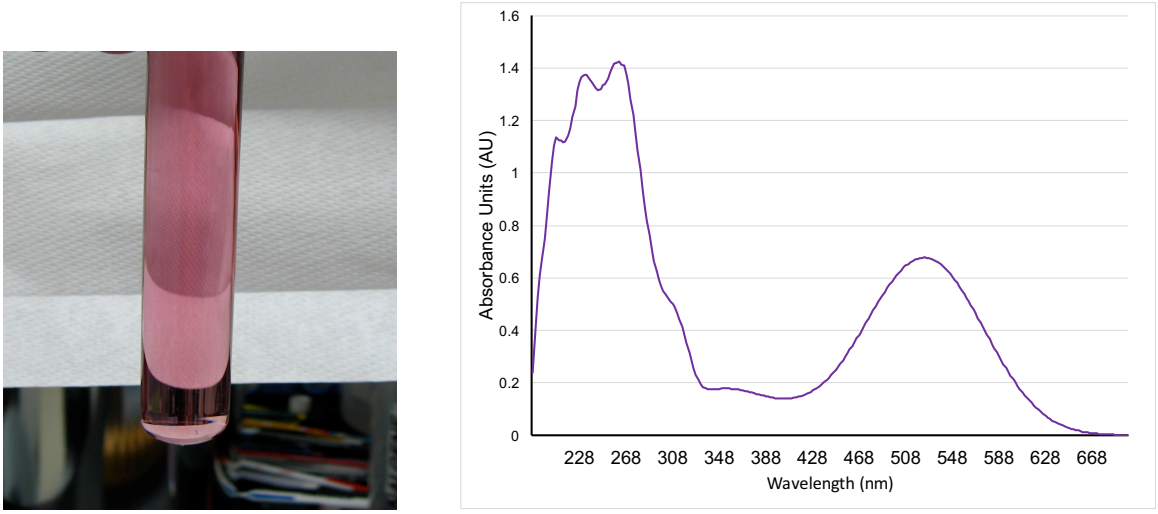

Supplementary Figure 3. **Color of fumisoquin C.** Photograph of a test tube (18 x 150 mm) from large-scale reverse-phase chromatography containing ~0.02 mg/mL of fumisoquin C, **3**, (left) and UV-Vis spectrum from HPLC-UV-MS analysis (right).

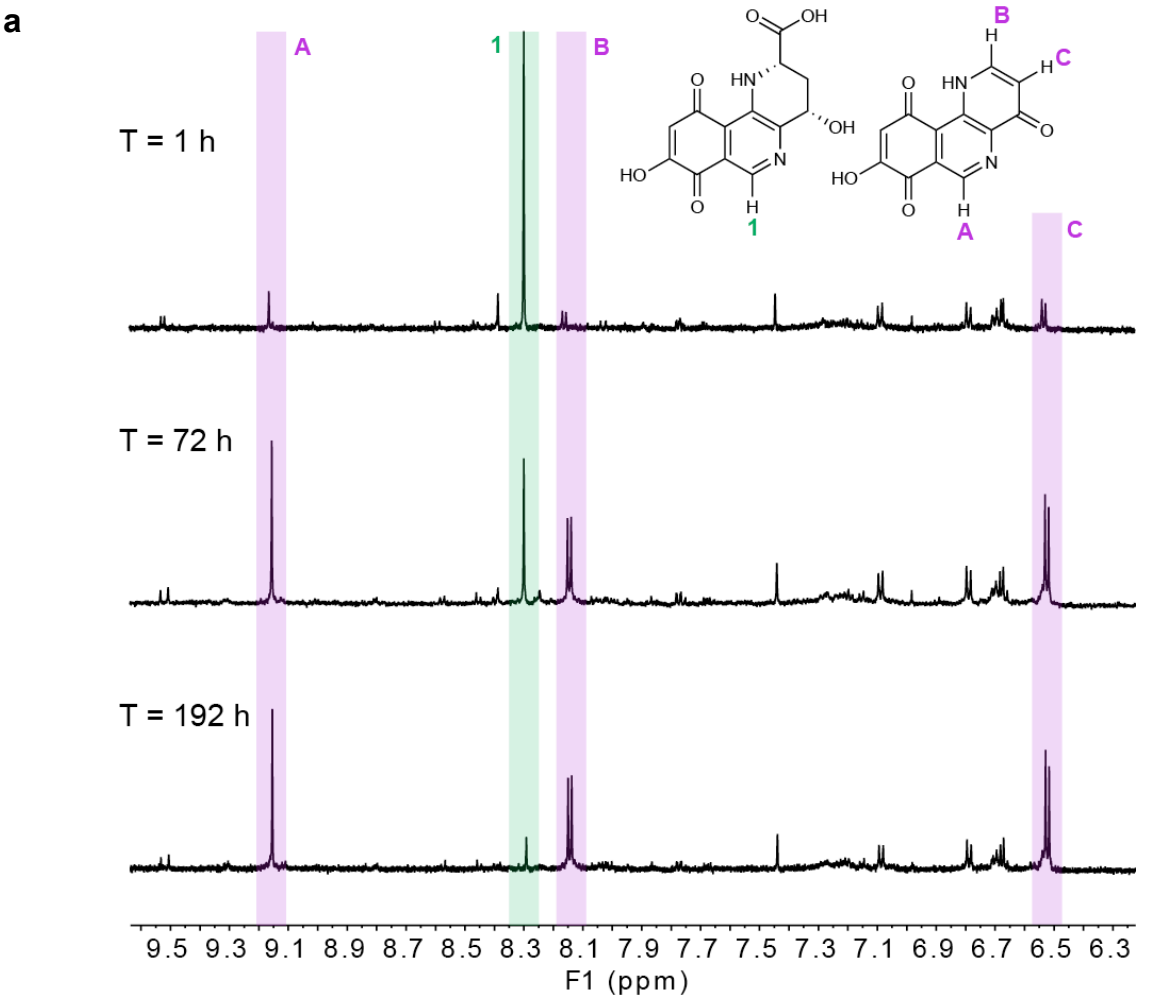

Supplementary Figure 4. **Fumisoquin C decomposition and derivatization.** (**a**) ^{1}H NMR spectra in CD_3OD at T = 2 h (top), T = 72 h (middle), and T = 192 h (bottom) after chromatographic purification, showing conversion of fumisoquin C, **3**, into **4**. (**b**) Conversion of fumisoquin C (**3**) into dimethyl fumisoquin C**.** See Online Methods for experimental procedure.

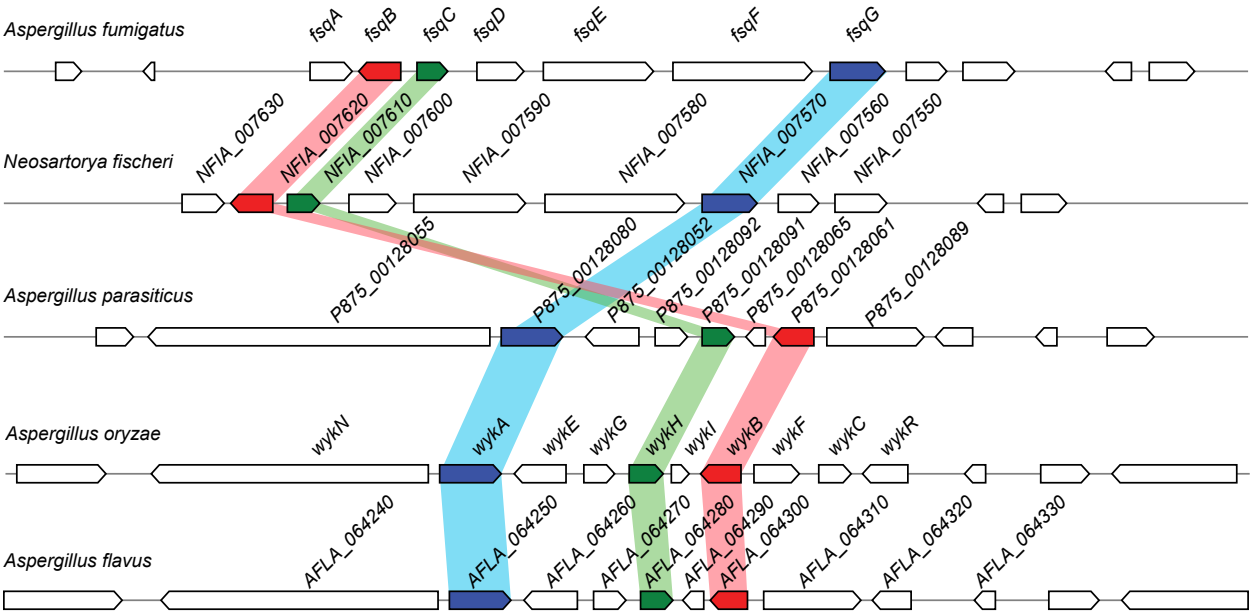

Supplementary Figure 5. Synteny analysis of *fsq* cluster in indicated *Aspergillus* and *Neosartorya* species. The analysis shows conservation of *fsqB* (red), *fsqC* (green), and *fsqG* (blue), which encode the enzymes responsible for the incorporation of the isoquinoline ring in **1-5**, and **18**. For % identity of these genes in each species shown, see **Supplementary Table 2**.

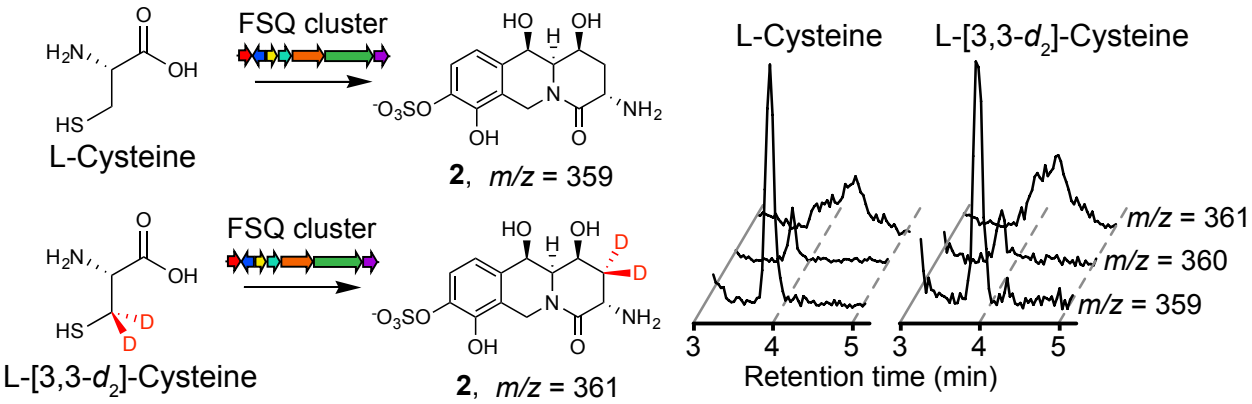

Supplementary Figure 6. **L-cysteine is not incorporated into the fumisoquins.** Ion chromatograms from HPLC-MS analysis of extracts from OE::*fsqA* fed with L-cysteine or L-[3,3-d_2]-cysteine. Indicated *m/z* values correspond to isotopomers of **2** with or without heavy atom incorporation.

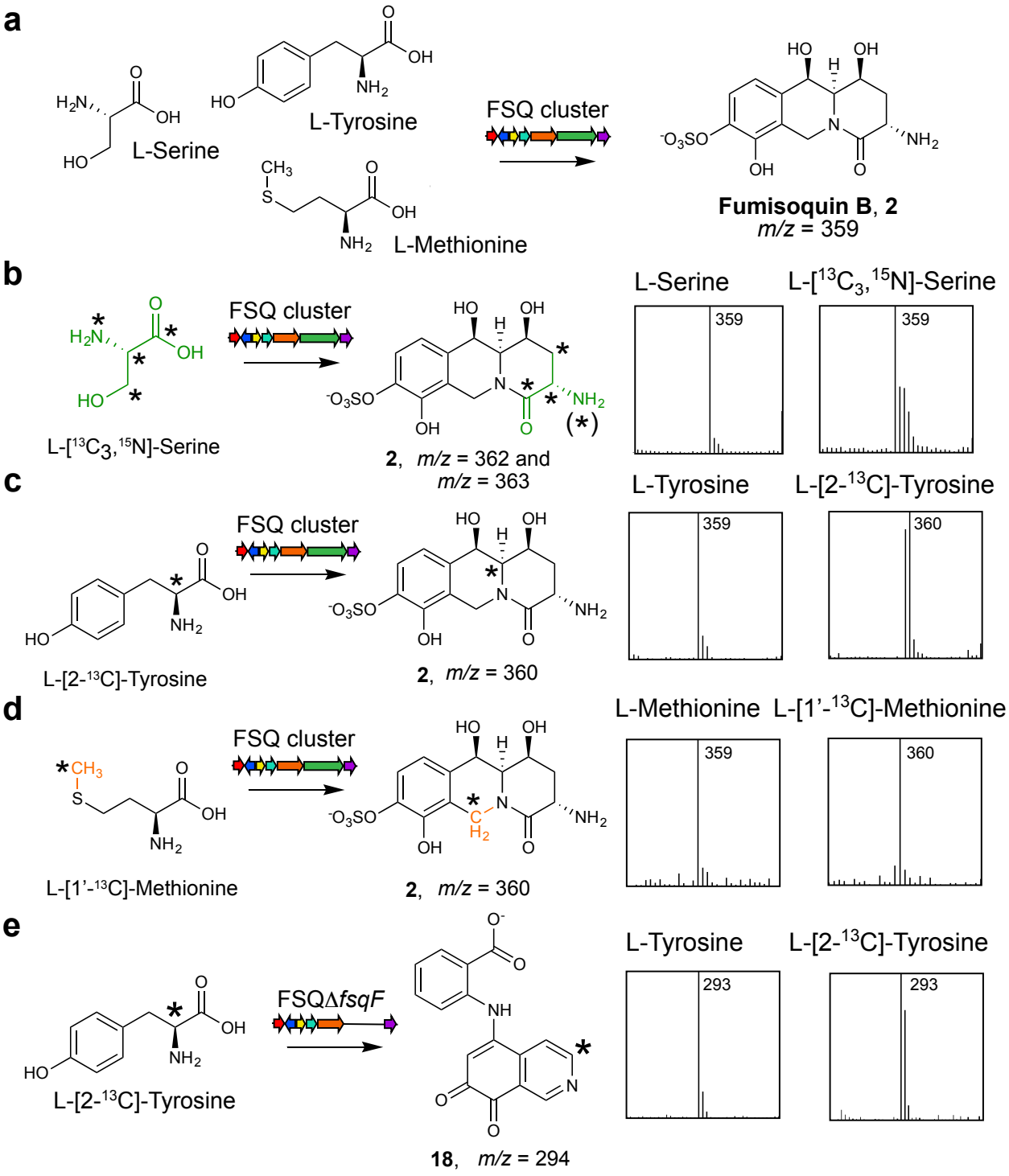

Supplementary Figure 7. **Mass spectra of FSQ cluster metabolites with and with out heavy atom incorporation**. (**a**) L-serine, L-tyrosine, and L-methionine are incorporated into the fumisoquins. (**b**) Mass spectrum of **2** with L-serine incorporated (left) and mass spectrum of **2** with L-[$^{13}C_3$, ^{15}N]-serine incorporated (right). Increased M+1 and M+2 peaks likely result from amination/deamination and use of abundant labeled serine for methionine production. (**c**) Mass spectrum of **2** with L-tyrosine incorporated (left) and mass spectrum of **2** with L-[2-^{13}C]-tyrosine incorporated (right). (**d**) Mass spectrum of **2** with L-methionine incorporated (left) and mass spectrum of **2** with L-[1'-^{13}C]-methionine incorporated (right). (**e**) Mass spectrum of **18** with L-tyrosine incorporated (left) and mass spectrum of **18** with L-[2-^{13}C]-tyrosine incorporated (right).

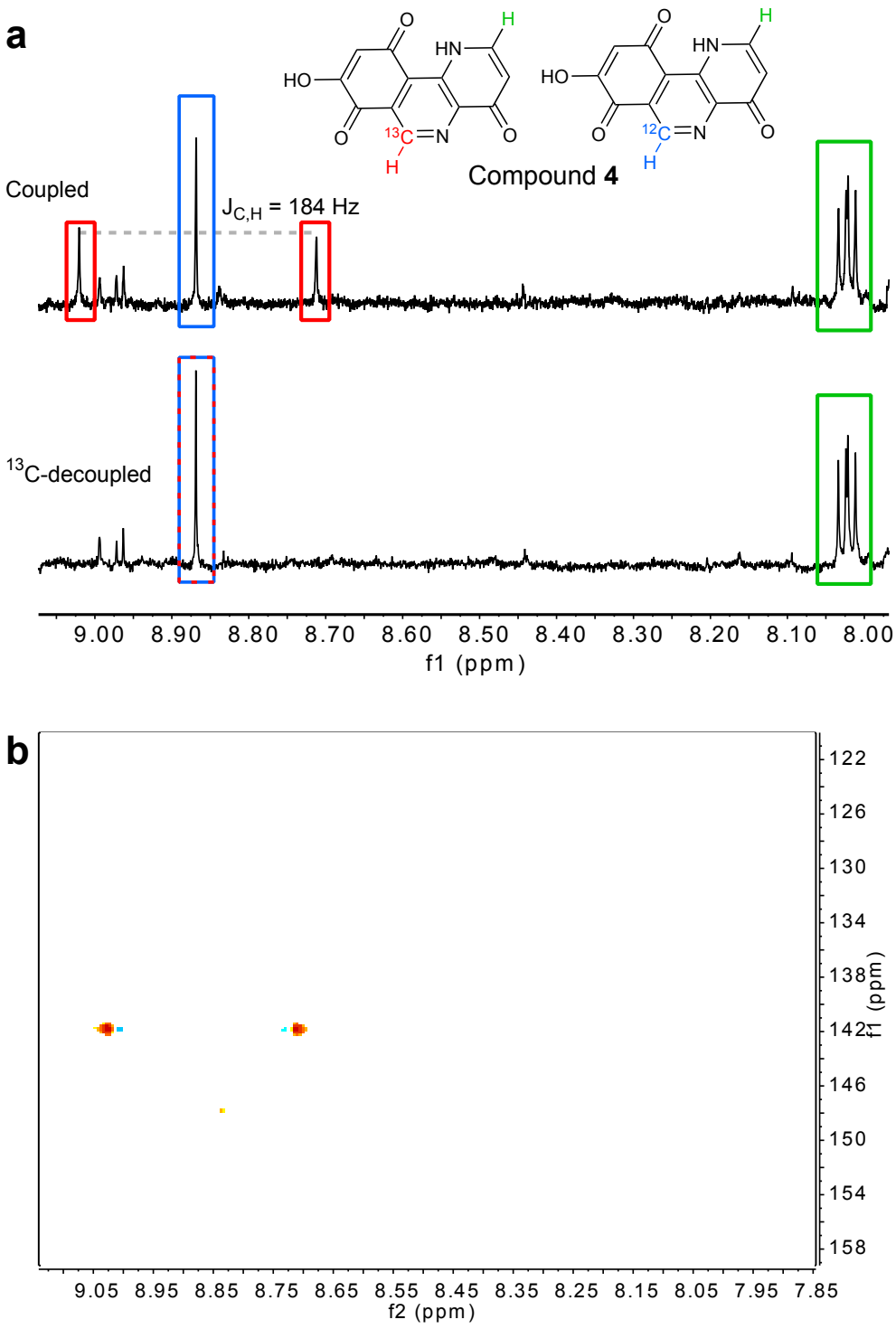

Supplementary Figure 8. **NMR spectra of ^{13}C-enriched 4** (a) ^{1}H-^{13}C coupled ^{1}H NMR spectrum of a sample of **4** obtained from fumisoquin C (**3**) isolated from a fungal culture grown with L-[1'-^{13}C]-methionine (top) and ^{1}H-^{13}C *decoupled* ^{1}H NMR spectrum of the same sample of **4** (bottom), showing selective incorporation of the methionine methyl group. In the decoupled spectrum, the intensity of the signal of the proton attached to the labeled carbon does not increase proportionally due to partial signal loss and line shape changes during decoupling. (**b**) ^{1}H-^{13}C coupled HSQC spectrum of this sample of **4**. Spectra were acquired using the 600 MHz Varian INOVA spectrometer, using DMSO-d_6 as solvent.

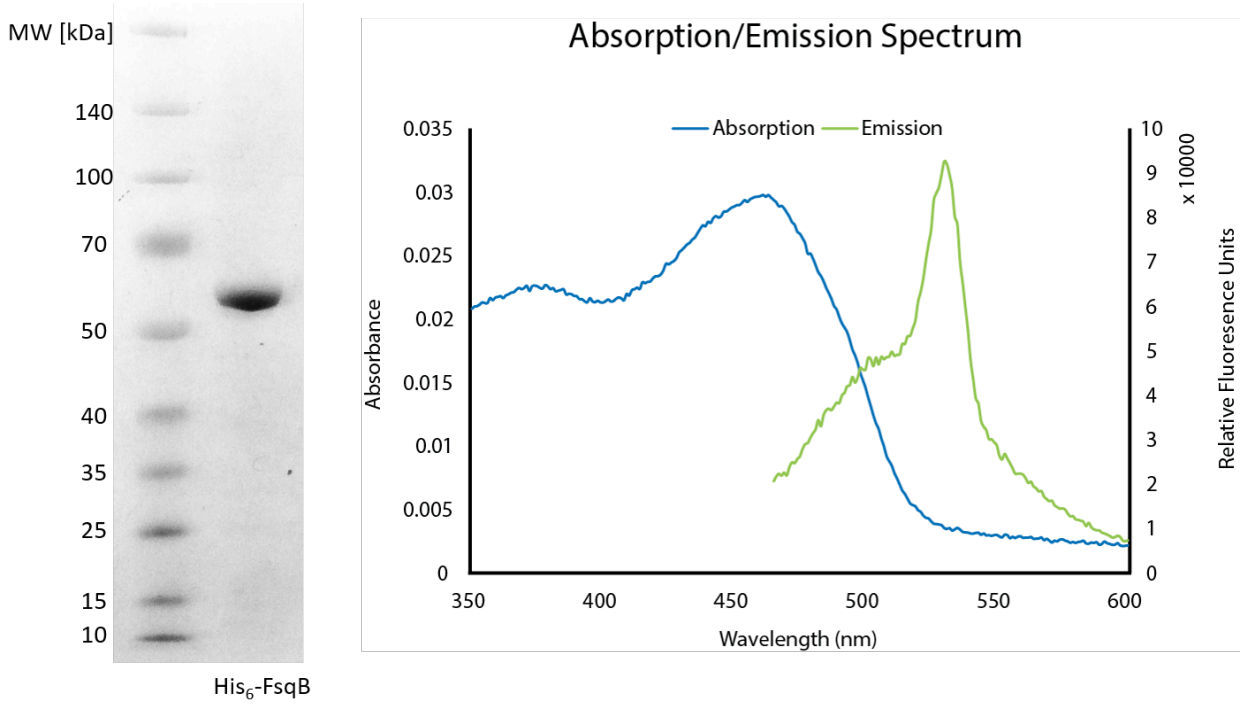

Supplementary Figure 9. **Purification and spectra of FsqB.** SDS-polyacrylamide gel of the polyhistidine-tagged FsqB (left), and UV-Vis absorption and fluorescence spectra (right) of FsqB. Spectra were acquired in 100 mM potassium phosphate buffer at pH 7.0, and fluorescence spectrum was acquired using an excitation wavelength of 450 nm.

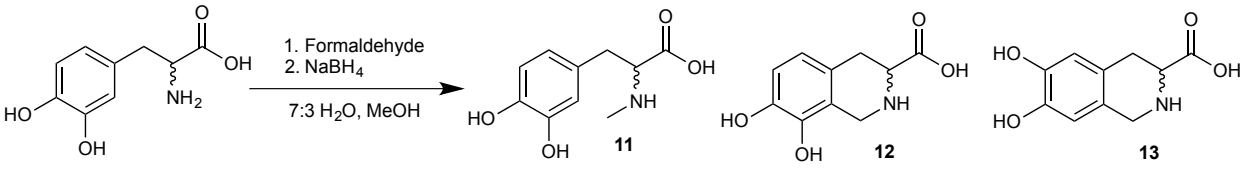

Supplementary Figure 10. Reaction of DL-DOPA with formaldehyde followed by addition of sodium borohydride produces a 7:3 mixture of cyclized products **12** and **13**, respectively, in addition to variable amounts of uncyclized **11**, as determined by HPLC-MS**.**

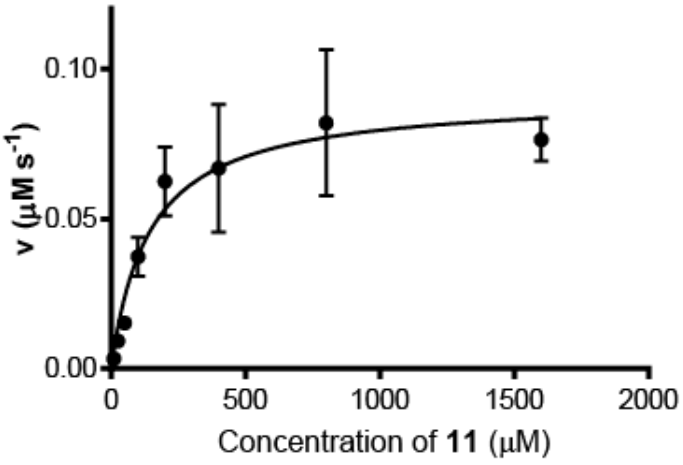

Supplementary Figure 11. **Enzymatic activity of FsqB.** Steady-state kinetics evaluated for FsqB on model substrate **11**. The observed apparent steady-state kinetic parameters of FsqB operating on **11** were K_M: 142.5 ± 42.9 μM and k_{cat}: 0.9 ± 0.1 s^{-1} at 25 °C. Each initial concentration of **11** was sampled twice for kinetic analysis, and displayed as the mean ± s.d.

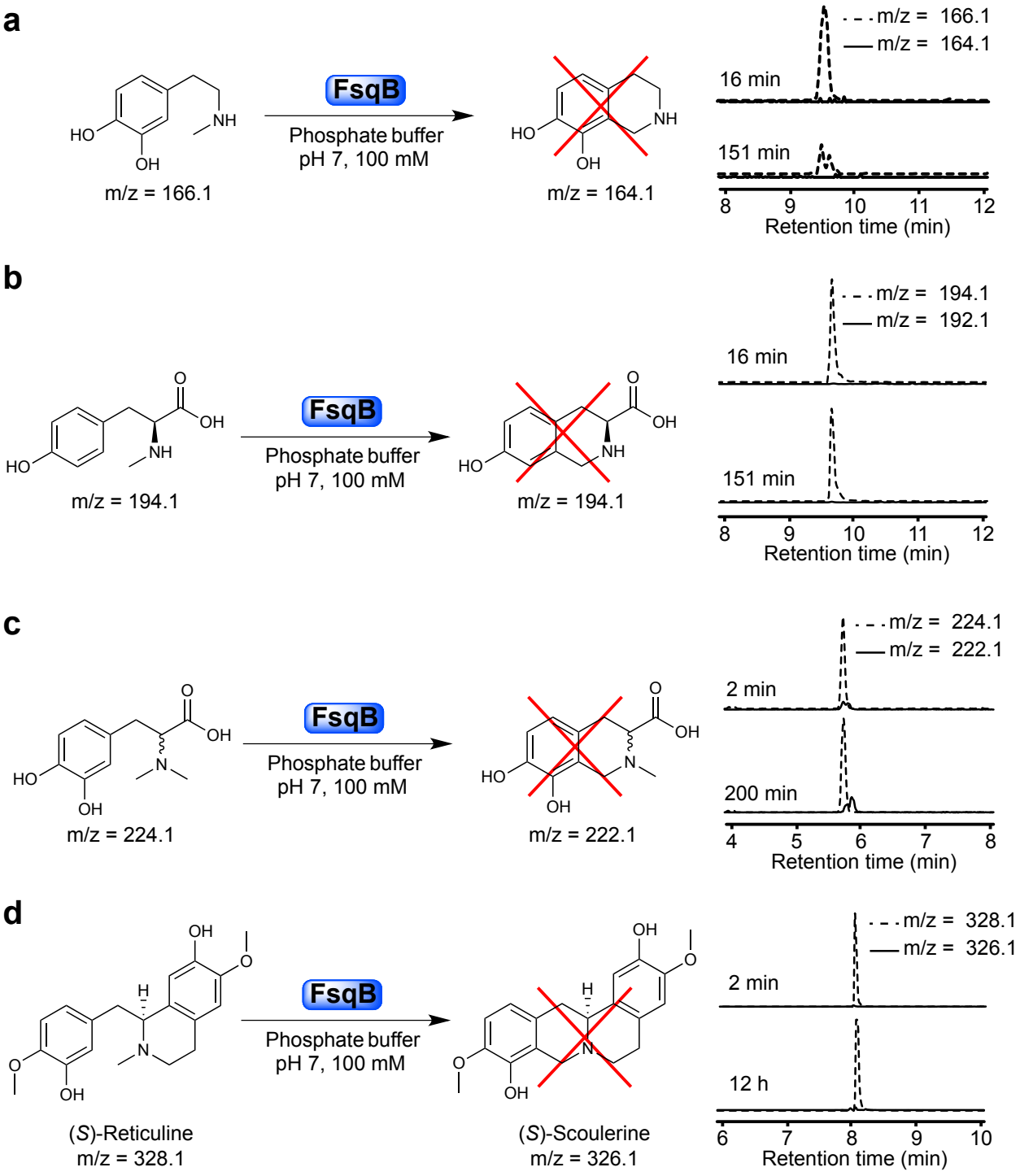

Supplementary Figure 12. Substrate specificity of FsqB. (**a**) Ion chromatograms for *N*-methyl dopamine (*m/z* = 166.1) and cyclic product (*m/z* = 164.1), showing no product formation after 151 min. (**b**) FsqB does not catalyze the cyclization of *N*-methyl-L-tyrosine. Ion chromatograms for *N*-methyl-L-tyrosine (*m/z* = 194.1) and cyclic product (*m/z* = 192.1) obtained after 151 min show no product formation. (**c**) FsqB does not catalyze the cyclization of *N,N*-dimethyl DOPA. Ion chromatograms for *N,N*-dimethyl DOPA (*m/z* = 224.1) and putative cyclic product (*m/z* = 222.1) obtained after 200 min show no product formation. Validating FsqB preference toward secondary β-*N*-methylamine substrates. (**d**) FsqB does not catalyze the cyclization of (*S*)-reticuline. Ion chromatograms for (*S*)-reticuline (*m/z* = 328.1) and cyclic product (*m/z* = 326.1) obtained after 12 h show no product formation.

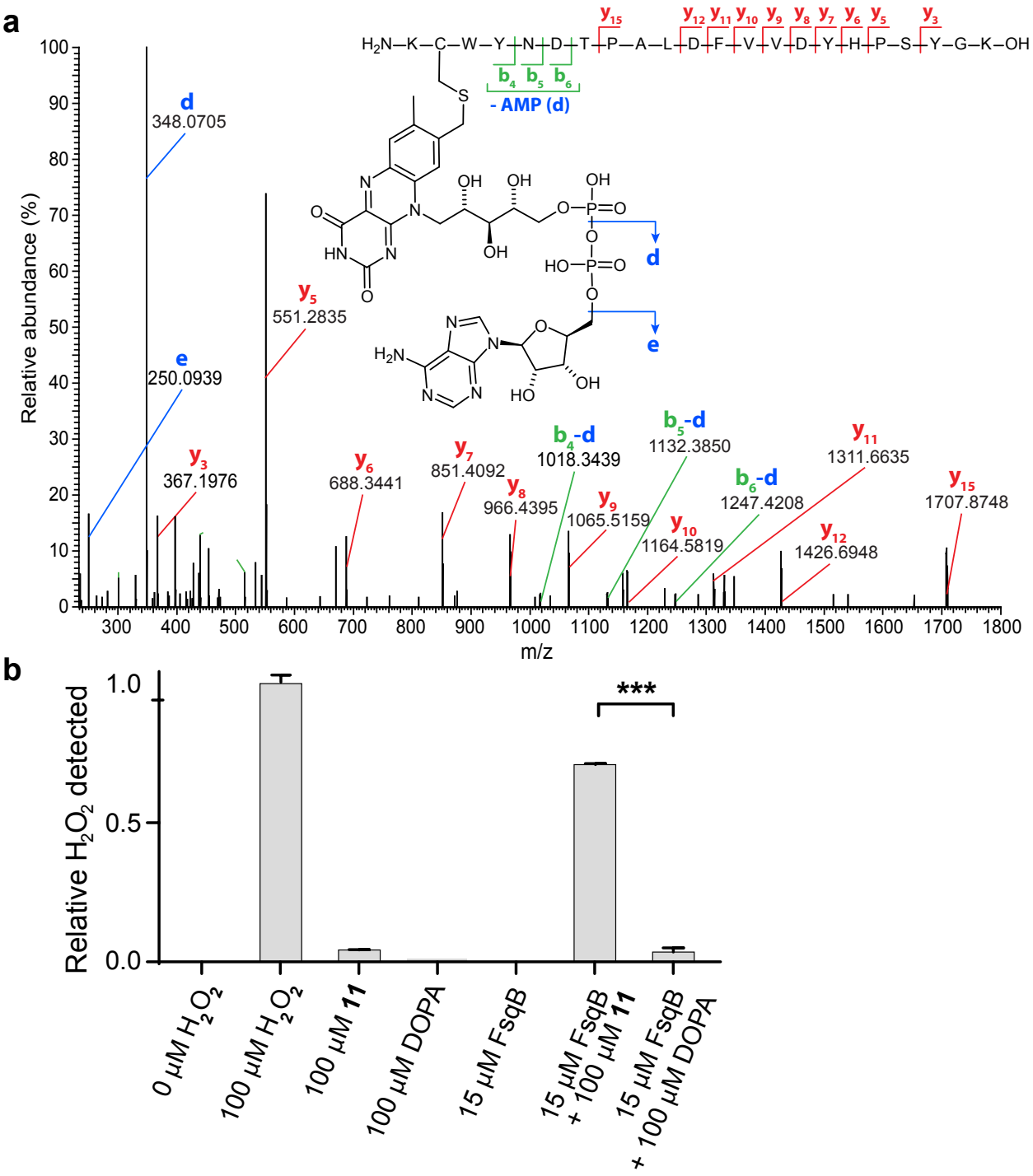

Supplementary Figure 13. **FsqB features a covalently bound FAD cofactor and produces H_2O_2 in the presence of substrate** (**a**) Collision-induced dissociation mass spectrum of tryptic FsqB peptide, revealing covalently bound FAD. Amino acid sequence and location of FAD attachment were inferred from indicated *b*- (green) and *y*-type (red) ion series and diagnostic FAD fragmentation (blue). (**b**) Amplex Red H_2O_2 assay of 15 μM FsqB with or without **11**, or 3,4-dihydroxy-DL-phenylalanine (DOPA) (100 mM phoshate buffer, pH 7, 1.5 h). Values were normalized to 0 and 100 μM H_2O_2 and presented as mean ± s.d. (n = 3), where * $P < 0.05$, ** $P < 0.001$, *** $P < 0.0001$, determined using Student's *t*-test.

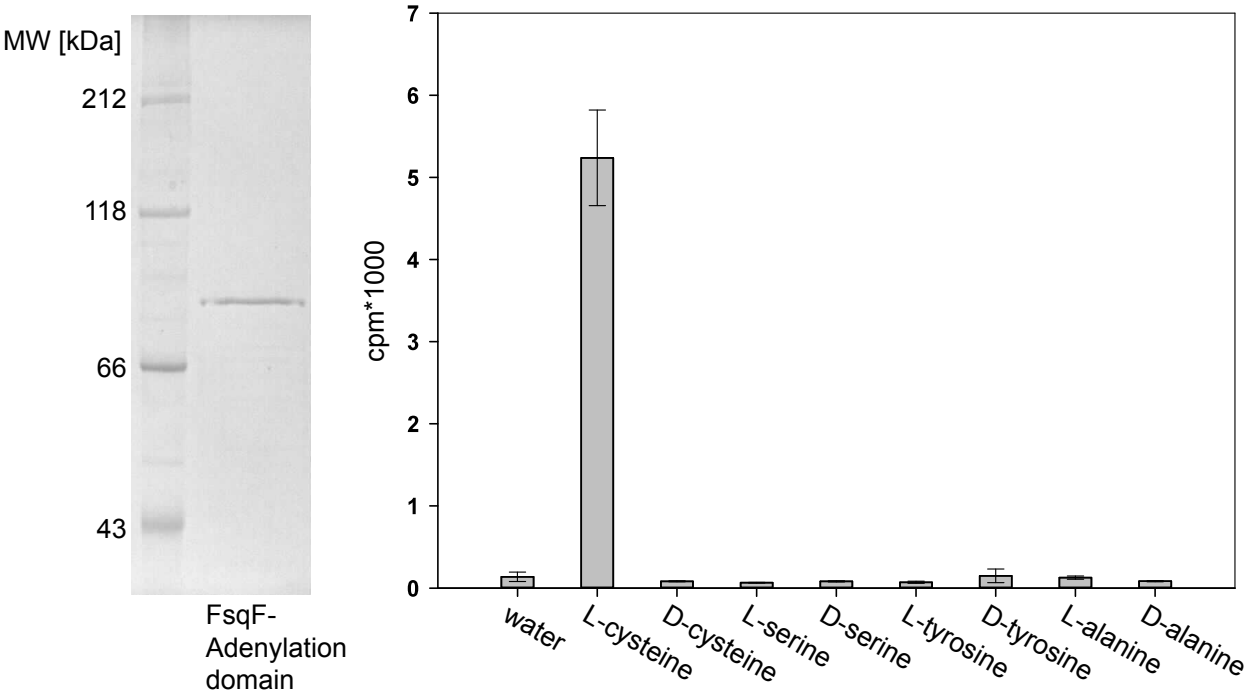

Supplementary Figure 14. **Properties of recombinant FsqF adenylation domain.** SDS-polyacrylamide gel showing the purity of the FsqF adenylation domain (left), and ATP-[^{32}P]pyrophosphate exchange assay results (right) for amino acids selected based on results from the stable-isotope labeling experiments (see **Fig. 4a-c** and **Supplementary Fig. 6** and Online Methods). The exchange assay shows none or minimal (in the case of L-cysteine) activation for all tested amino acids. Collectively, the assay results suggest that no standard amino acid is the true substrate, but rather a derivative of an amino acid, such as dehydroalanine, as proposed in the biosynthetic model shown in main text **Fig. 3**.

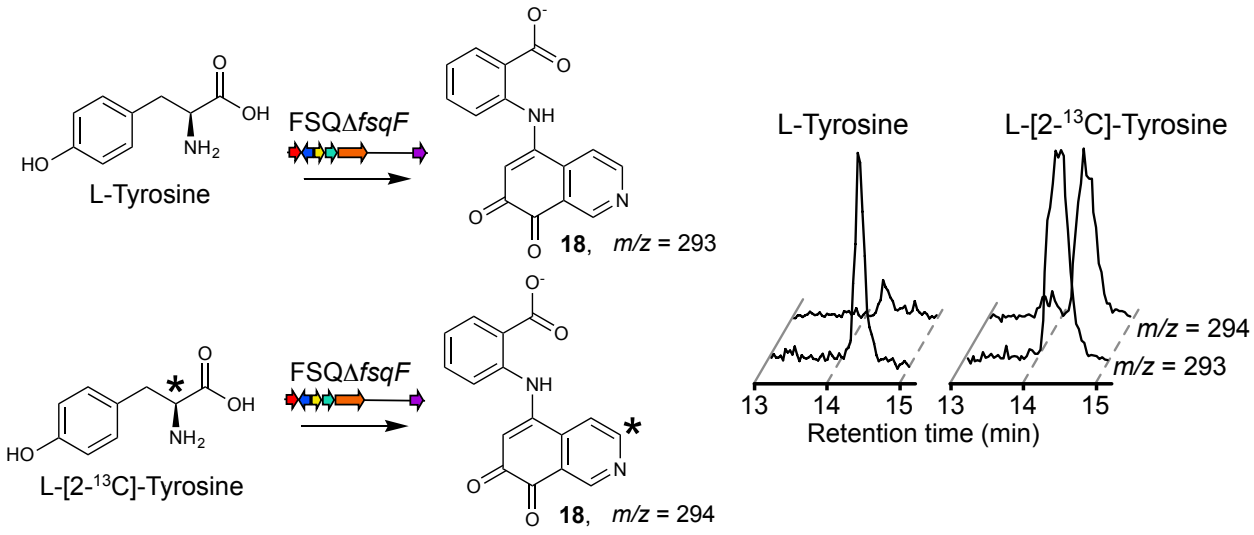

Supplementary Figure 15. **L-tyrosine is incorporated into shunt metabolite 18.** Ion chromatograms extracted from HPLC-MS analysis of extracts from OE::*fsqA*-Δ*fsqF* fed with L-tyrosine or L-[2-^{13}C]-tyrosine. The indicated *m/z* values correspond to **18** with or without heavy atom incorporation. The data support the hypothesis that FsqD is responsible for incorporation of L-tyrosine and not FsqF, as shown in main text **Fig 3.**

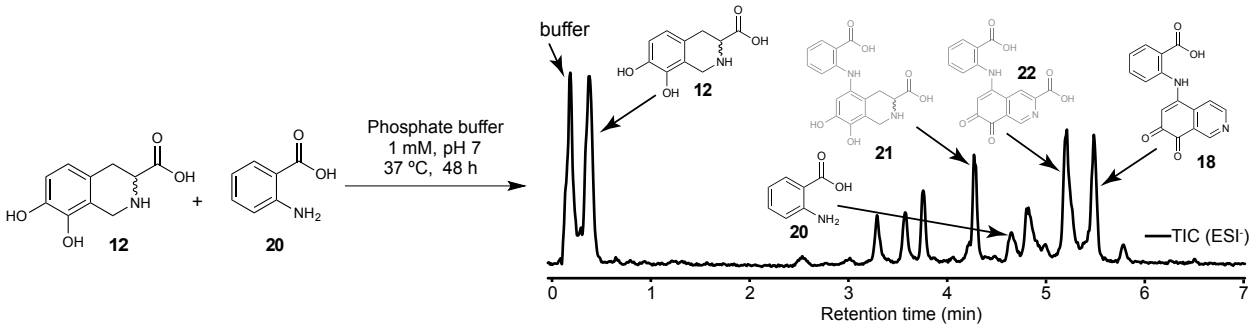

Supplementary Figure 16. Shunt metabolite 18 is produced non-enzymatically from 12 and anthranilic acid, 20. High-resolution UHPLC-MS total ion chromatogram for a reaction mixture of **12** and **20** reveals formation of **18**, along with two intermediates, **21** and **22** (proposed structures shown in gray). See **Supplementary Table 1** for HRMS data.

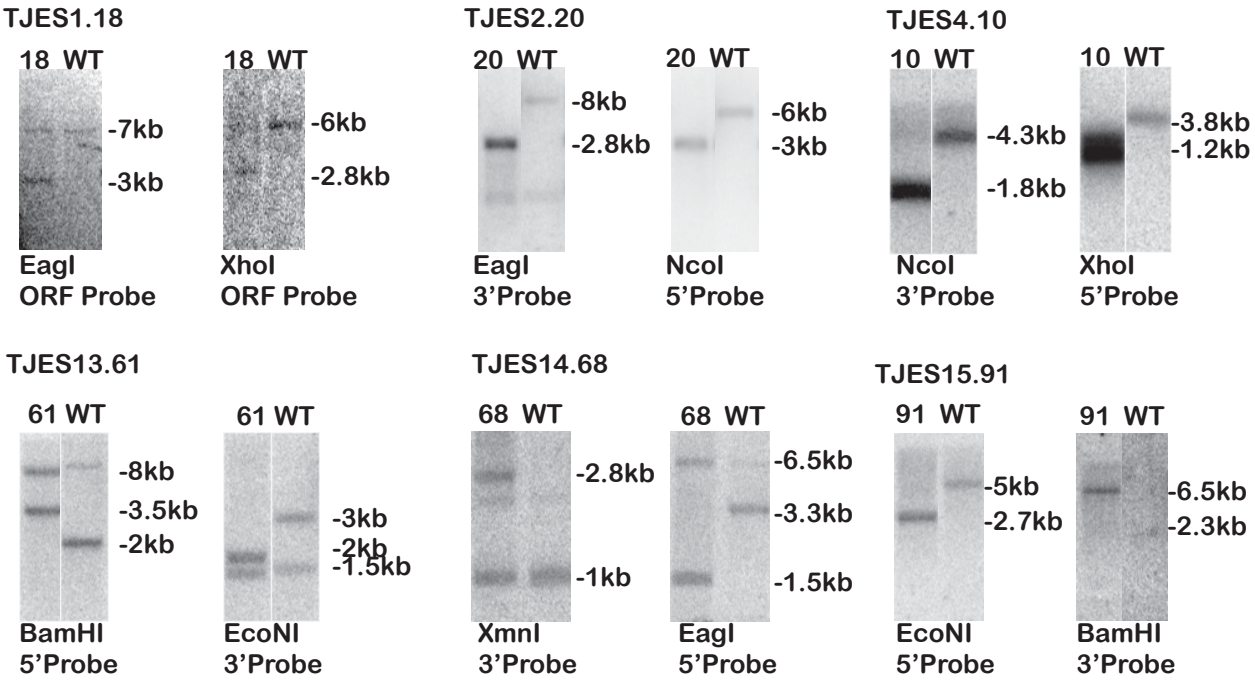

Supplementary Figure 17. Southern analysis confirmation of all mutants used in this study. Mutant (number) lanes are on the left of each image and the parental strain ("WT") is shown on the right. Expected band sizes correlating with those seen in the images are marked accordingly. Under each image is the enzymes used in the restriction digest as well as the nucleic acid probe us

Supplementary References

1. Clauser, K. R., Baker, P. & Burlingame, A. L. Role of accurate mass measurement (+/- 10 ppm) in protein identification strategies employing MS or MS/MS and database searching. *Anal Chem* **71,** 2871–82 (1999).

2. Xue, T., Nguyen, C. K., Romans, A., Kontoyiannis, D. P. & May, G. S. Isogenic auxotrophic mutant strains in the Aspergillus fumigatus genome reference strain AF293. *Arch Microbiol* **182,** 346-353 (2004).

3. He, Z., Price, M.S., OBrian, G.R., Georgianna, D.R. & Payne, G.A. Improved protocols for functional analysis in the pathogenic fungus Aspergillus flavus. *BMC Microbiology* **7**, 104 (2007).

4. Palmer, J. M. *et al.* Loss of CclA, required for histone 3 lysine 4 methylation, decreases growth but increases secondary metabolite production in Aspergillus fumigatus. *PeerJ* **1**, e4 (2013).

5. Sekonyela, R. *et al.* RsmA regulates Aspergillus fumigatus gliotoxin cluster metabolites including cyclo(L-Phe-L-Ser), a potential new diagnostic marker for invasive aspergillosis. *PLoS One* **8**, e62591 (2013).

6. Lim, F.Y., *et al.* Genome-Based Cluster Deletion Reveals an Endocrin Biosynthetic Pathway in Aspergillus fumigatus. *Appl Environ Microbiol* **78**, 4117-4125 (2012).

7. Calvo, A.M., Bok, J.W., Brooks, W. & Keller, N.P. LeA Is Required for Toxin and Sclerotial Production in Aspergillus parasiticus. *Appl Environ Microbiol* **70**, 4733-4739 (2004)

Supplementary Note

^{1}H (800 MHz) and ^{13}C (200 MHz) NMR spectroscopic data for fumisoquin A, 1, in methanol-d_4.

Chemical shifts were referenced to δ(C<u>H</u>D_2OD) = 3.31 and δ(^{13}<u>C</u>HD_2OD) = 49.0.^{13}C chemical shifts were determined via HMBC and HSQC spectra. ^{1}H, ^{1}H-*J*-coupling constants were determined from the acquired ^{1}H or dqfCOSY spectra. NOESY correlations were observed using a mixing time of 400 ms. HMBC correlations are from the proton(s) stated to the indicated ^{13}C atom.

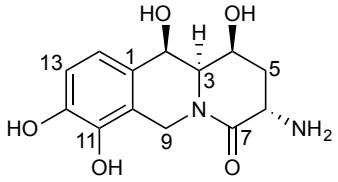

No.	δ_c	Proton	δH (J_{HH}[Hz])	HMBC	NOESY
1	128.03				
2	70.99	2-H	4.94 ($J_{2,3}$ = 1.9)	1, 3, 4, 7, 10, 11, 14	3, 4, 14
3	60.44	3-H	3.73 ($J_{3,2}$ = 1.9, $J_{3,4}$ = 8.7)	1, 7	2, 4, 5b
4	67.19	4-H	4.65 ($J_{4,3}$ = 8.7, $J_{4,5a}$ = 7.6, $J_{4,5b}$ < 1)	5	2, 5a, 5b
5	33.67	5-H_a	2.46 ($J_{5a,4}$ = 7.6, $J_{5a,5b}$ = 13.0, $J_{5a,6}$ = 5.7)	3, 4, 6, 7	4, 6, 5b
		5-H_b	2.06 ($J_{5b,4}$ < 1, $J_{5b,5a}$ = 13.0, $J_{5b,6}$ = 12.4)	3, 4, 6, 7	3, 4, 5a
6	47.88	6-H	4.29 ($J_{6,5a}$ = 5.7, $J_{6,5b}$ = 12.4)	5, 7	5a
7	169.75				
8					
9	42.35	9-H_a	4.66 ($J_{9Ha,9Hb}$ = 18.0)	1, 2, 3, 6, 7, 10, 11, 12, 13	
		9-H_b	4.78 ($J_{9Hb,9Ha}$ = 18.0)	1, 2, 3, 6, 7, 10, 11, 12, 13	3
10	119.92				
11	142.82				
12	146.06				
13	114.23	13-H	6.73 ($J_{13,14}$ = 8.0)	1, 10, 11, 12	14
14	120.04	14-H	6.70 ($J_{14,13}$ = 8.0)	1, 2, 4, 9, 10, 12, 13	2,1 3

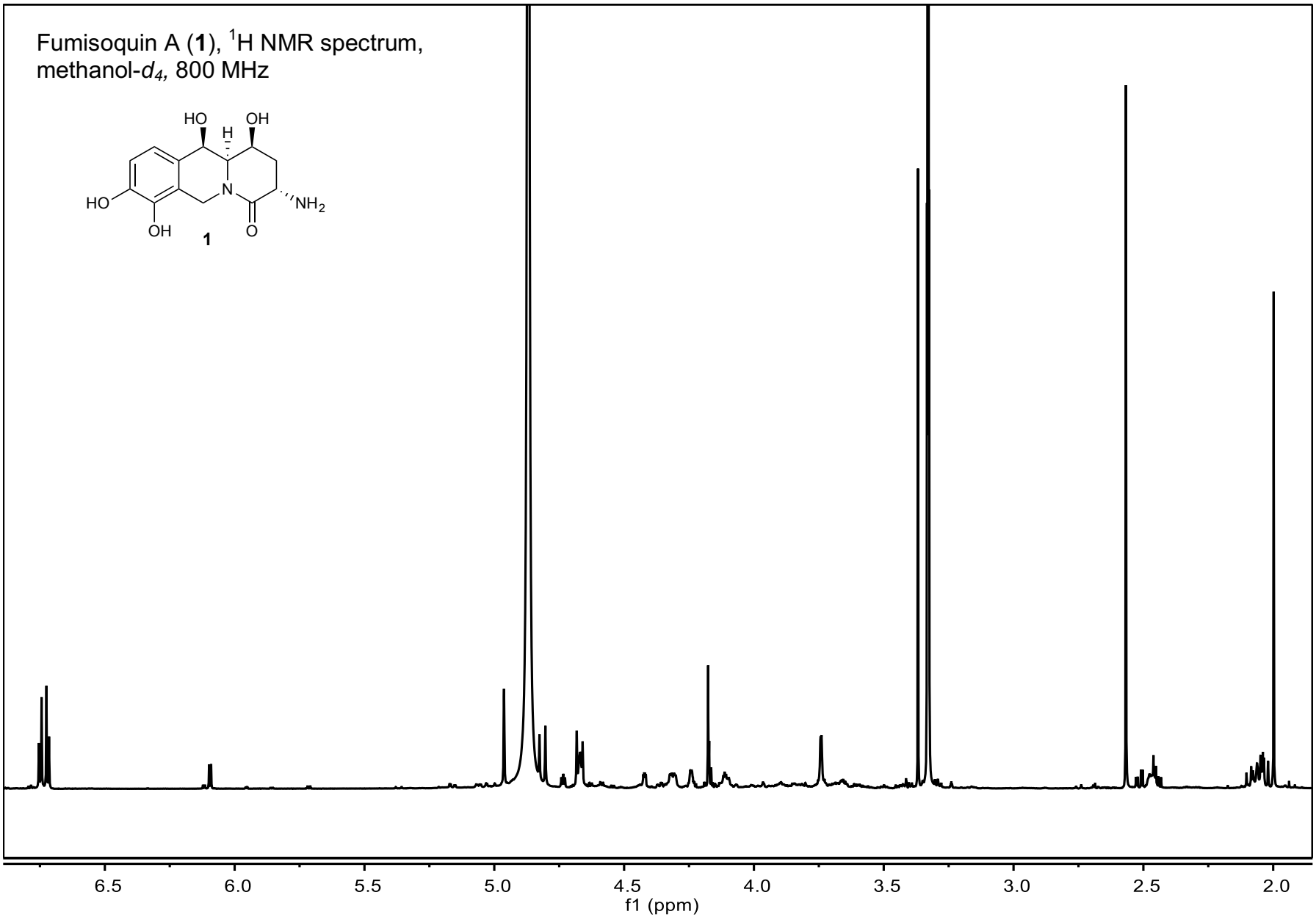
Fumisoquin A (1), ^{1}H NMR spectrum,
methanol-d_4, 800 MHz
HO
OH
H
HO
OH
N
NH2
O
1
6.5
6.0
5.5
5.0
4.5
4.0
3.5
3.0
2.5
2.0
f1 (ppm)

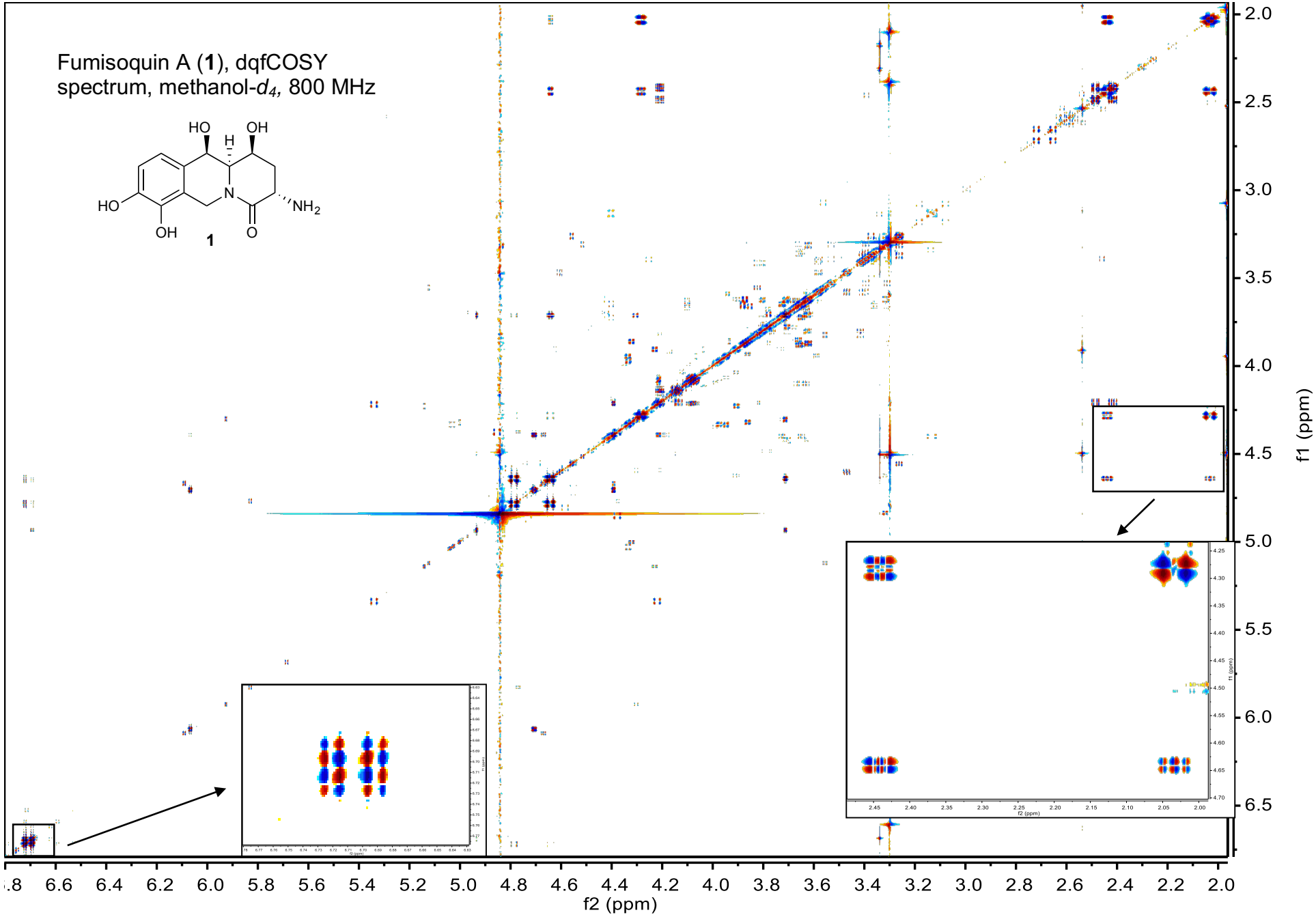
Fumisoquin A (1), dqfCOSY spectrum, methanol-d_4, 800 MHz
HO
H
OH
HO
N
NH_2
OH
O
1
f2 (ppm)
f1 (ppm)

Fumisoquin A (**1**), coupled HSQC spectrum, methanol-d_4, 800 MHz

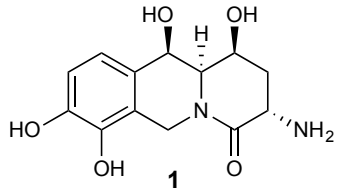

1

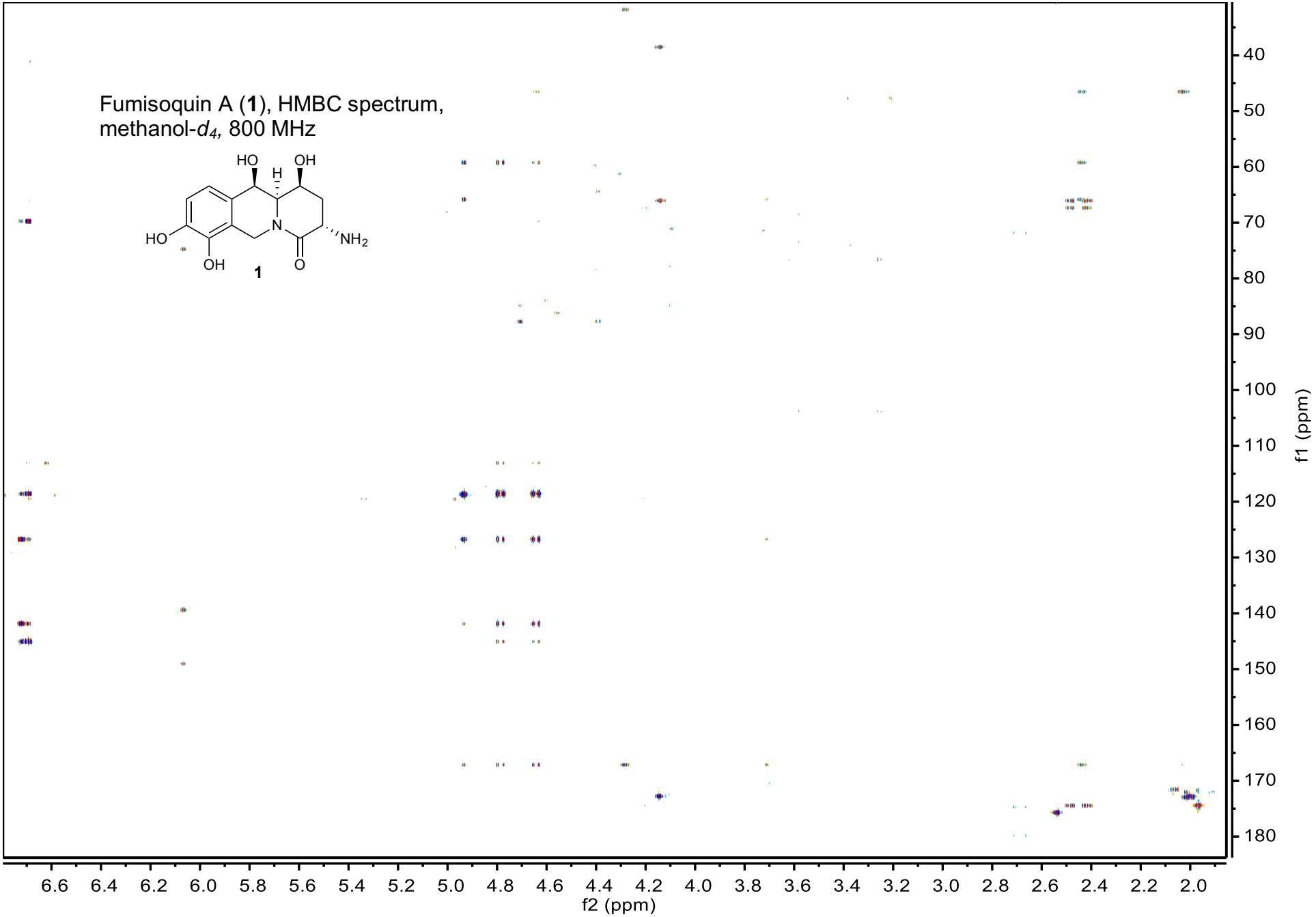
Fumisoquin A (1), HMBC spectrum,
methanol-d4, 800 MHz
HO
H
OH
HO
N
NH2
OH
O
1
40
50
60
70
80
90
100
110
120
130
140
150
160
170
180
f1 (ppm)
6.6
6.4
6.2
6.0
5.8
5.6
5.4
5.2
5.0
4.8
4.6
4.4
4.2
4.0
3.8
3.6
3.4
3.2
3.0
2.8
2.6
2.4
2.2
2.0
f2 (ppm)

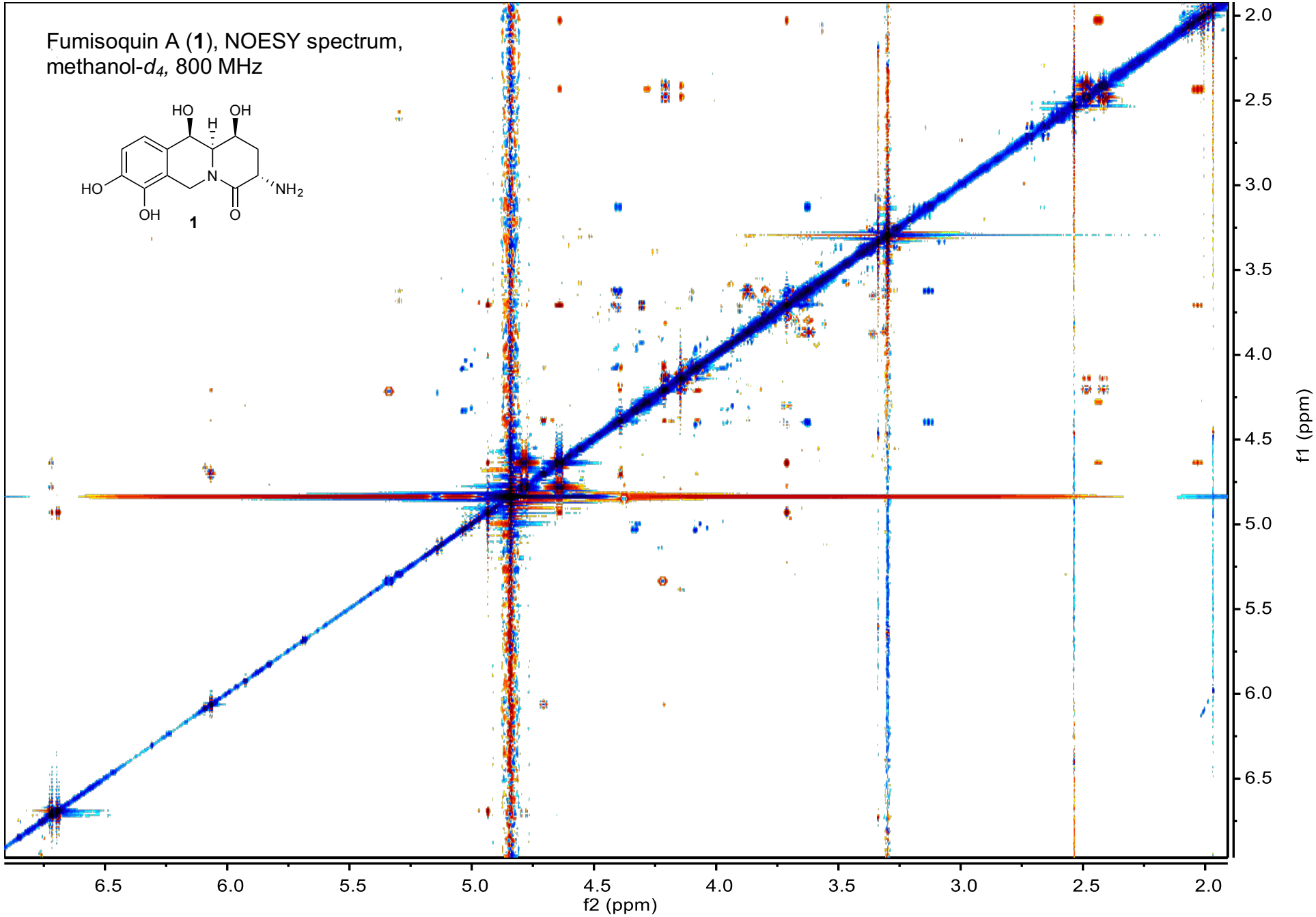
Fumisoquin A (1), NOESY spectrum,
methanol-d4, 800 MHz
HO
OH
H
HO
OH
N
NH2
O
1
f2 (ppm)
f1 (ppm)
6.5
6.0
5.5
5.0
4.5
4.0
3.5
3.0
2.5
2.0

^{1}H (600 MHz) and ^{13}C (151 MHz) NMR spectroscopic data for fumisoquin B, 2, in methanol-d_4.

Chemical shifts were referenced to δ(C<u>H</u>D_2OD) = 3.31 and δ(^{13}<u>C</u>HD_2OD) = 49.0.^{13}C chemical shifts were determined via HMBC and HSQC spectra. ^{1}H, ^{1}H-*J*-coupling constants were determined from the acquired ^{1}H or dqfCOSY spectra. ROESY correlations were observed using a mixing time of 500 ms. HMBC correlations are from the proton(s) stated to the indicated ^{13}C atom.

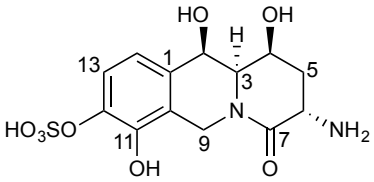

No.	δ_c	Proton	δH (J_{HH}[Hz])	HMBC[a]	ROESY
1	134.03				
2	70.75	2-H	4.98 ($J_{2,3}$ = 2.0)	1, 3, 10	4, 14
3	60.19	3-H	3.71 ($J_{3,2}$ = 2.0, $J_{3,4}$ = 9.2)		5a
4	67.30	4-H	4.62 ($J_{4,3}$ = 9.2, $J_{4,5a}$ = 6.9, $J_{4,5b}$ = 7.9)	6	2
5	34.69	5-H_a	1.94 ($J_{5a,4}$ = 6.9, $J_{5a,5b}$ = 13.0, $J_{5a,6}$ = 11.5)	4, 6, 7	3
		5-H_b	2.43 ($J_{5b,4}$ = 7.9, $J_{5b,5a}$ = 13.0, $J_{5b,6}$ = 5.8)	4, 6, 7	
6	47.88	6-H	4.02 ($J_{6,5a}$ =11.5, $J_{6,Hb}$ = 5.8)	5, 7	
7	171.61				
8					
9	42.26	9-H_a	4.63 ($J_{9Ha,9Hb}$ = 18.5)	3	
		9-H_b	4.81 ($J_{9Hb,9Ha}$ = 18.5)	10, 11	
10	121.61				
11	147.05				
12	140.92				
13	122.08	13-H	7.23 ($J_{13,14}$ = 8.1)	1, 11, 12w	
14	119.96	14-H	6.83 ($J_{14,13}$ = 8.1)	2, 10, 12, 13	2

[a]w: weak correlation (less than ~10% of the intensity of strongest signal)

Metabolome fraction, containing fumisoquin B (**2**), ^{1}H NMR spectrum, methanol-d_4, 600 MHz

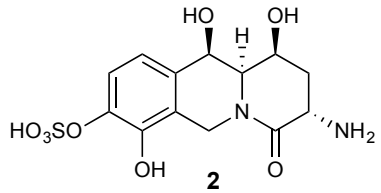

2

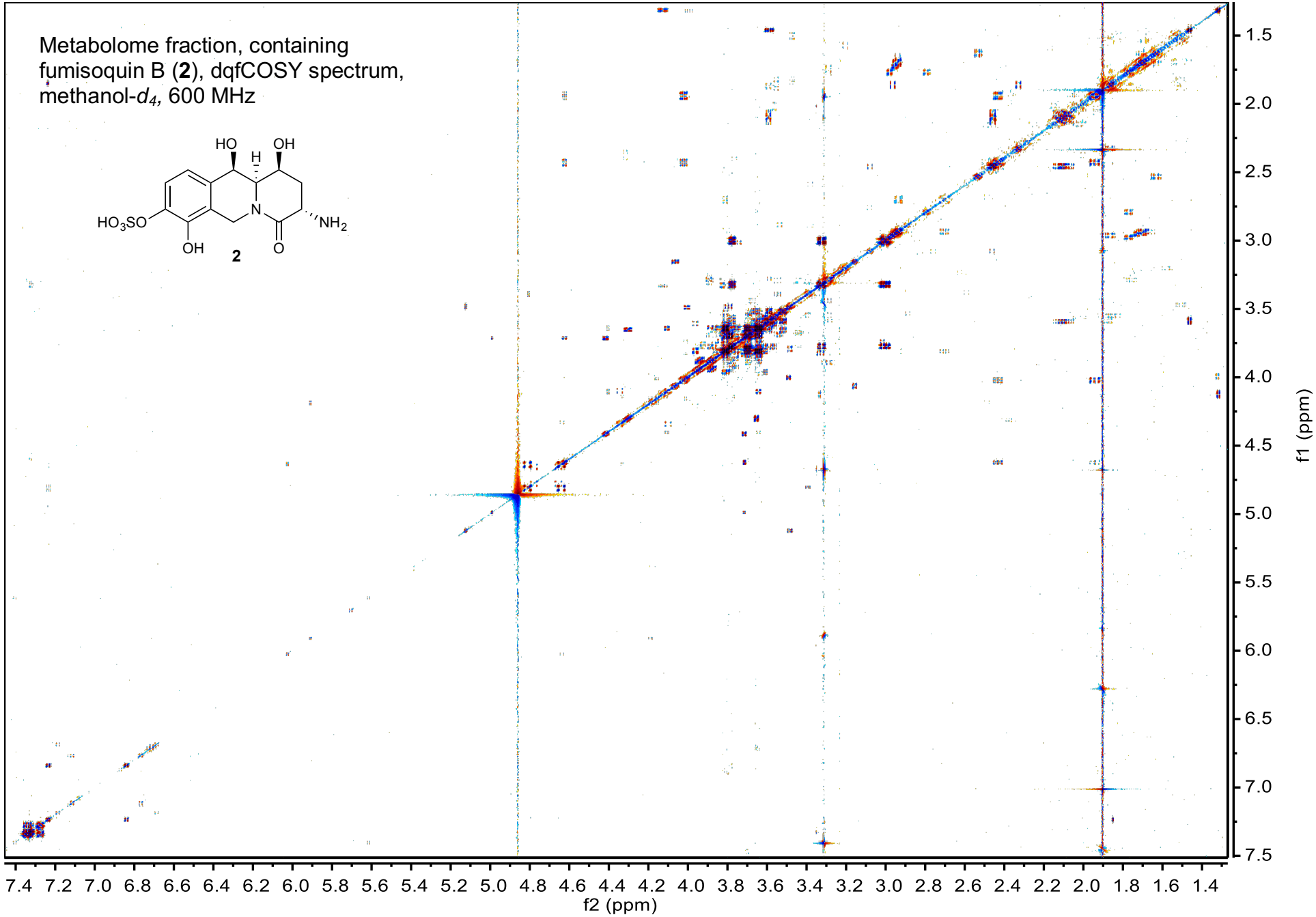
Metabolome fraction, containing fumisoquin B (2), dqfCOSY spectrum, methanol-d4, 600 MHz
HO
H
OH
HO3SO
N
NH2
OH
O
2
f2 (ppm)
f1 (ppm)

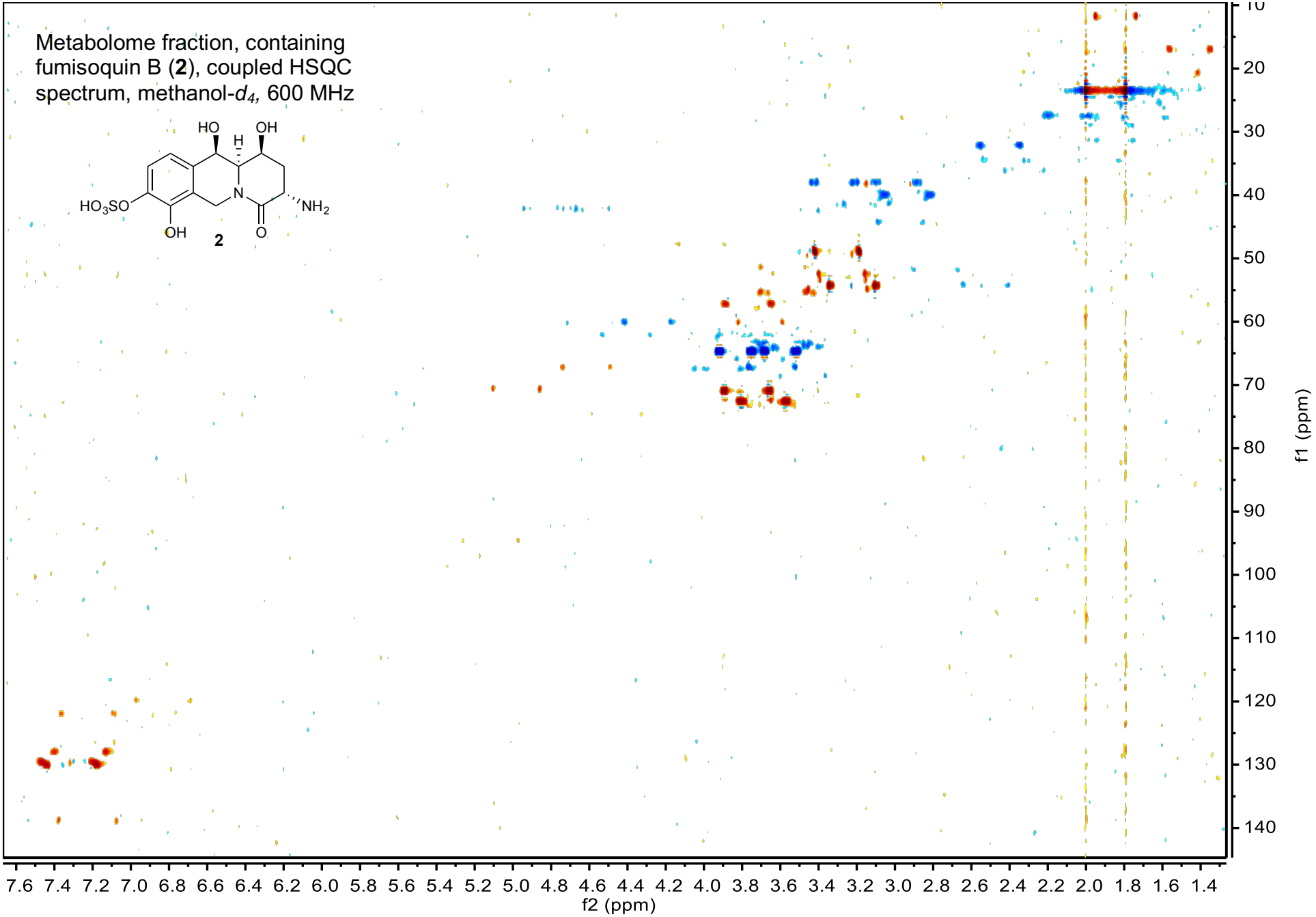
Metabolome fraction, containing fumisoquin B (2), coupled HSQC spectrum, methanol-d_4, 600 MHz
HO
H
OH
HO_3SO
N
NH_2
OH
O
2
f2 (ppm)
f1 (ppm)

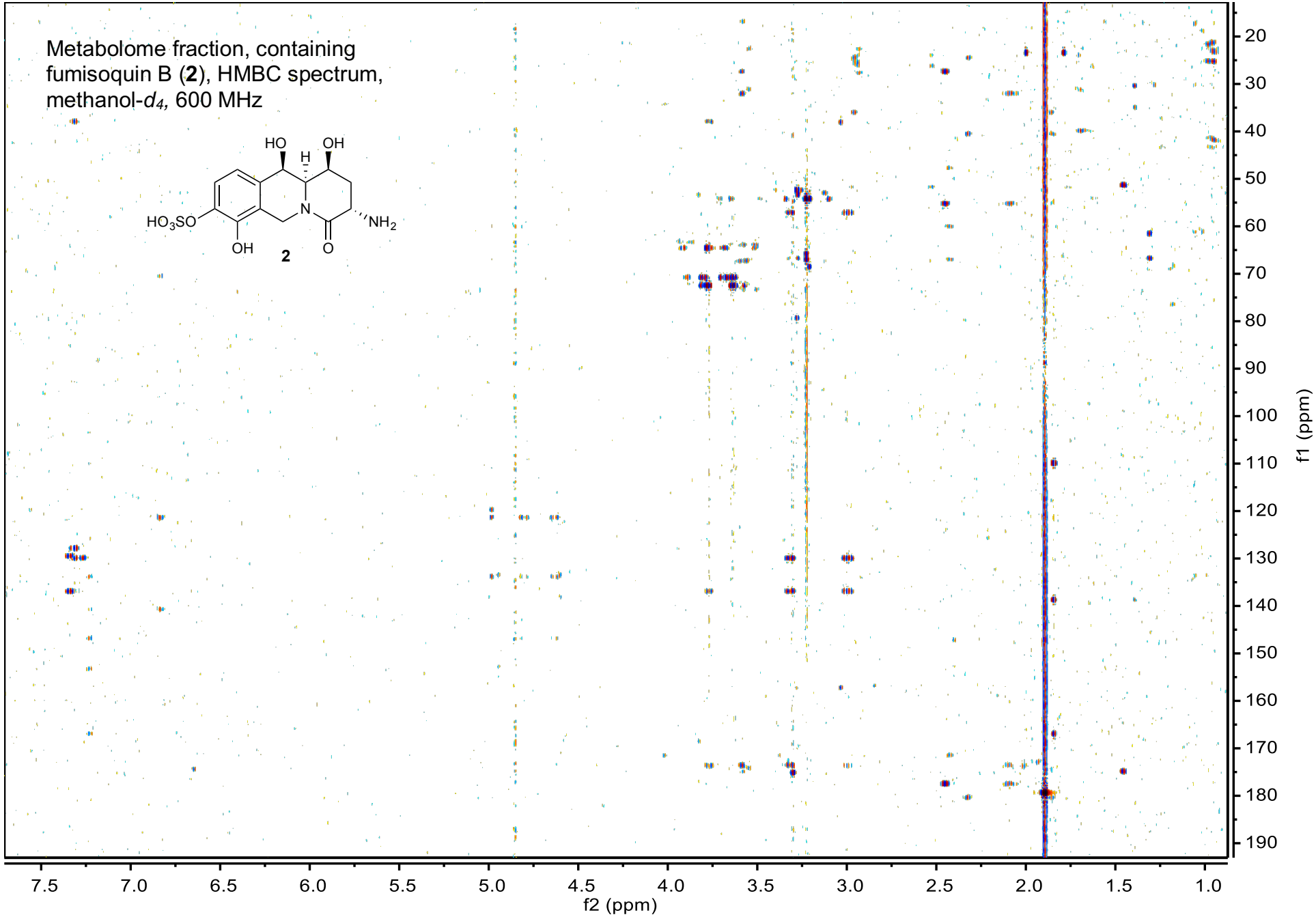
Metabolome fraction, containing
fumisoquin B (2), HMBC spectrum,
methanol-d4, 600 MHz
HO
OH
H
N
HO3SO
NH2
OH
O
2
f2 (ppm)
f1 (ppm)

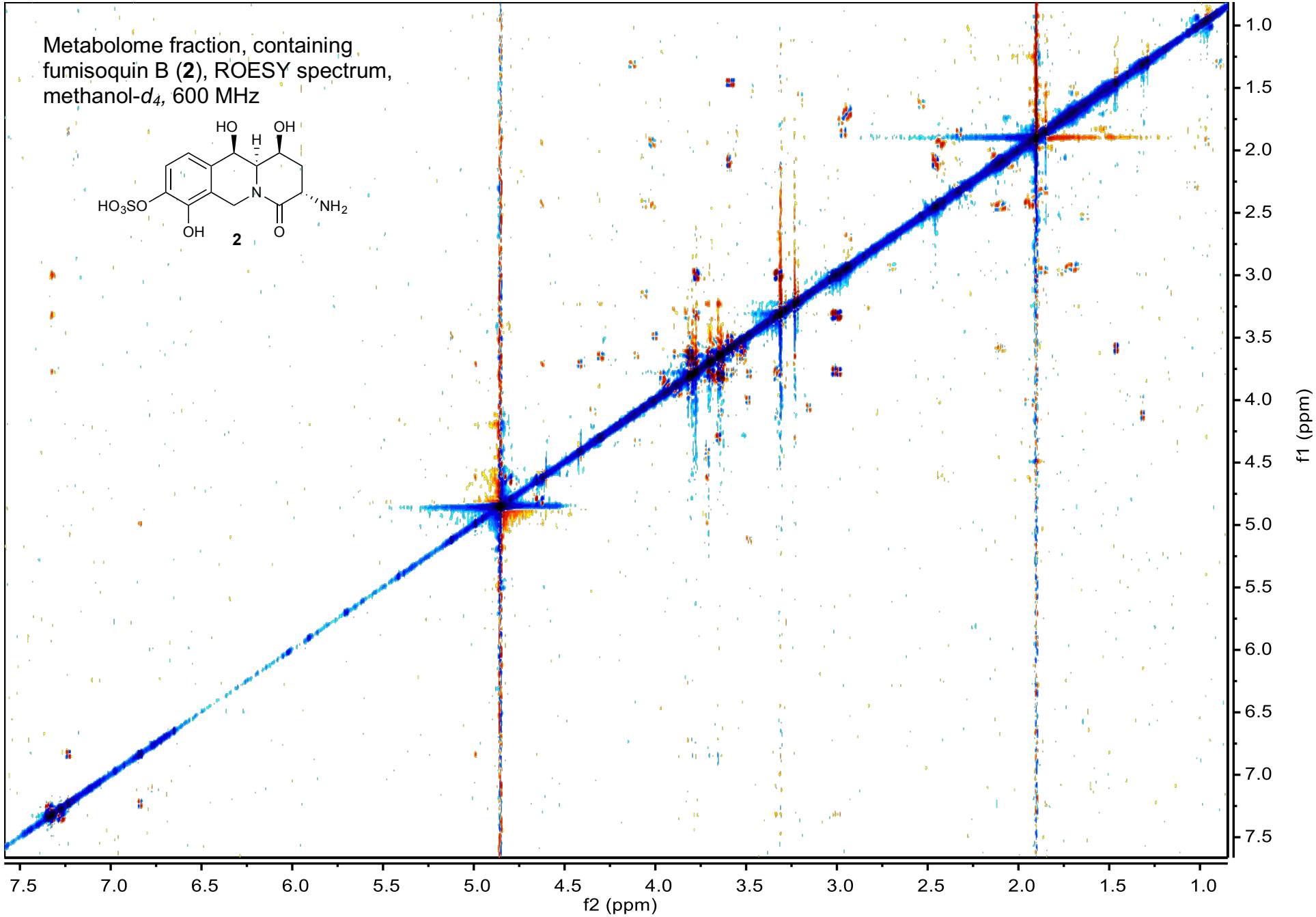
Metabolome fraction, containing
fumisoquin B (2), ROESY spectrum,
methanol-d4, 600 MHz
HO
H
OH
HO3SO
N
NH2
OH
O
2
f2 (ppm)
f1 (ppm)

^{1}H and ^{13}C spectroscopic data for fumisoquin C, 3, in DMSO-d_6.

Chemical shifts were referenced to δ(C<u>H</u>D_2SOCD_3) = 2.50 and δ(^{13}<u>C</u>HD_2SOCD_3) = 39.52. ^{13}C chemical shifts were determined via HMBC and HSQC spectra. Spectra were acquired using the Varian INOVA 600 spectrometer, except for the HSQC, which was acquired using the Bruker Avance 800 spectrometer. ^{1}H, ^{1}H-*J*-coupling constants were determined from the acquired ^{1}H spectrum. NOESY correlations were observed using a mixing time of 600 ms. HMBC correlations are from the proton(s) stated to the indicated ^{13}C atom.

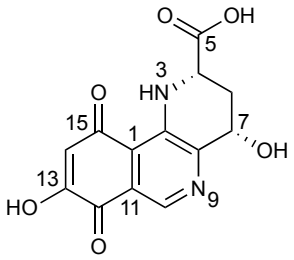

No.	δ_c	Proton	δH (J_{HH}[Hz])	HMBC	NOESY
1	115.62				
2	138.33				
3		3-NH	9.46 ($J_{3,4}$ = 1.5)	1, 4, 5, 6, 8	4
4	53.27	4-H	3.73 ($J_{4,3}$ = 1.5, $J_{4,6a}$ =9.6, $J_{4,6b}$ = 5.4)	2, 5, 6, 7	3, 7
5	173.40				
6	32.31	6-Ha	1.69 ($J_{6a,4}$ =12, $J_{6a,6b}$ = 12.8, $J_{6a,7}$ = 9.5)	4, 5, 7, 8	
		6-Hb	2.38 ($J_{6b,4}$ =12, $J_{6a,6b}$ = 12.8, $J_{6b,7}$ = 5.3)	4, 5, 7, 8	
7	66.85	7-H	4.57 ($J_{7,6a}$ = 9.5, $J_{7,6b}$ = 5.3)	2, 4, 6, 8	4
8	152.69				
9					
10	130.73	10-H	7.98	1, 8, 11, 12, 13, 15	
11	124.93				
12	188.04				
13[a]	184.60				
14	107.92	14-H	5.24	1, 12, 13, 15	
15[a]	170.85				

[a]Position 13 and 15 carbon chemical shifts are interchangeable

Fumisoquin C (**3**), containing about 40% of decomposition product **4,** ^{1}H NMR spectrum, methanol-d_4, 600 MHz

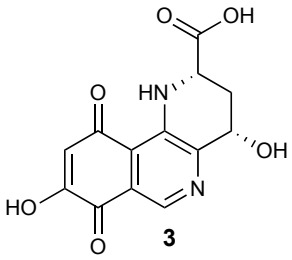

3

Fumisoquin C (**3**), containing about 40% of decomposition product **4,** dqfCOSY spectrum, methanol-d_4, 600 MHz

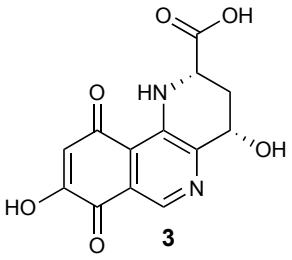

3

Fumisoquin C (**3**), containing about 40% of decomposition product **4,** ^{1}H NMR spectrum, DMSO-d_6, 600 MHz

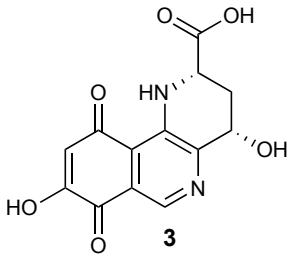

3

Fumisoquin C (**3**), containing about 40% of decomposition product **4**, coupled HSQC spectrum, DMSO-d_6, 800 MHz

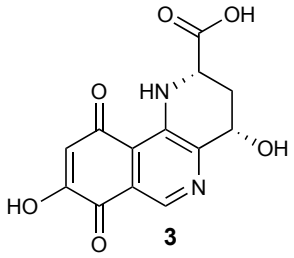

3

Fumisoquin C (**3**), containing about
40% of decomposition product **4**,
HMBC spectrum, DMSO-d_6, 600 MHz

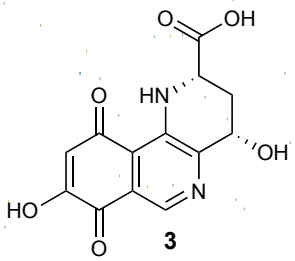

3

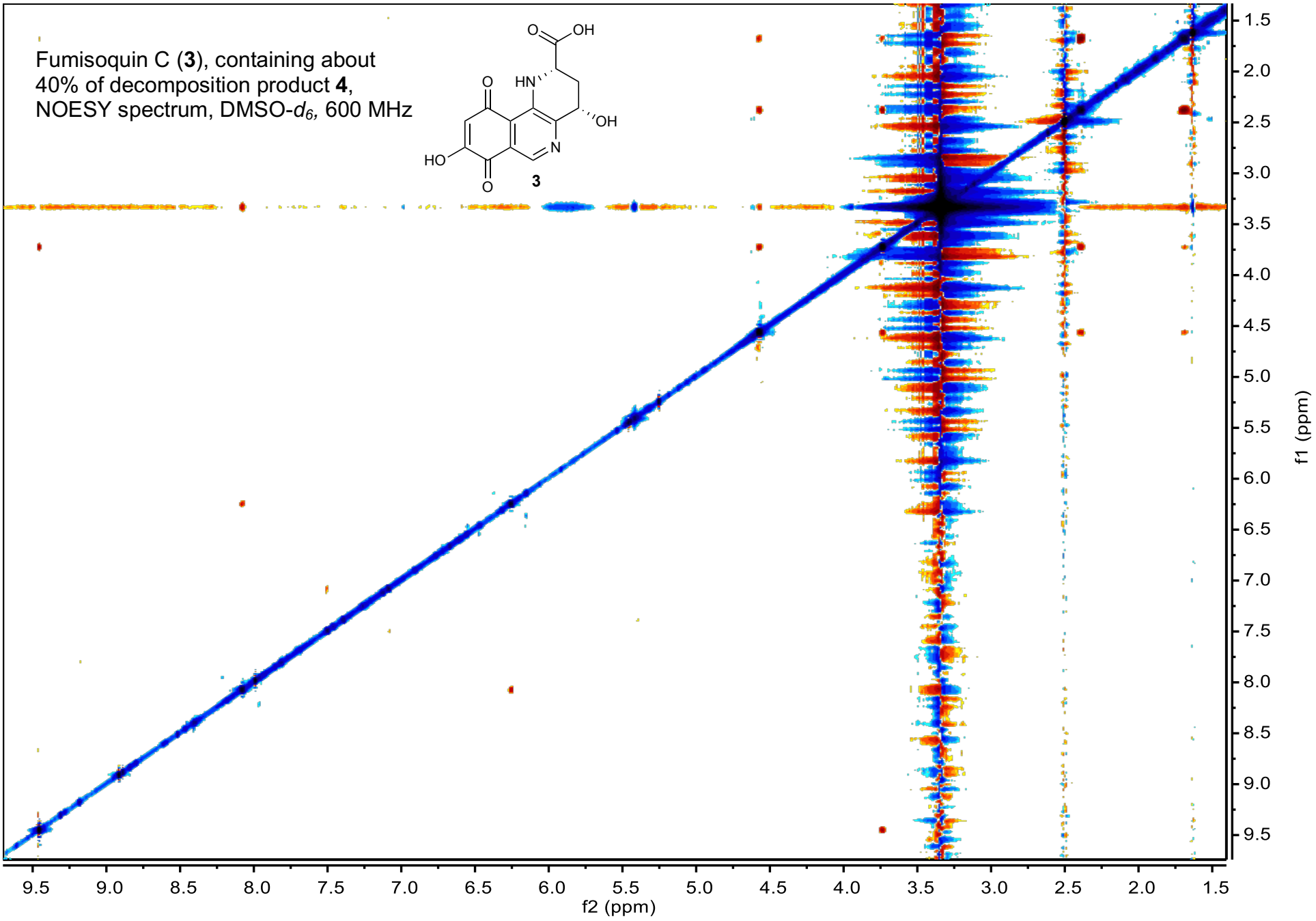
Fumisoquin C (3), containing about
40% of decomposition product 4,
NOESY spectrum, DMSO-d6, 600 MHz
O
OH
HN
OH
HO
N
O
3
9.5
9.0
8.5
8.0
7.5
7.0
6.5
6.0
5.5
5.0
4.5
4.0
3.5
3.0
2.5
2.0
1.5
f2 (ppm)
f1 (ppm)

^{1}H (800 MHz) and ^{13}C (200 MHz) NMR spectroscopic data for dimethyl-fumisoquin C (dimethyl-3) in DMSO-d_6.

Chemical shifts were referenced to δ(C<u>H</u>D$_2$SOCD$_3$) = 2.50 and δ(^{13}<u>C</u>HD$_2$SOCD$_3$) = 39.52. ^{13}C chemical shifts were determined via HMBC and HSQC spectra. ^{1}H, ^{1}H-*J*-coupling constants were determined from the acquired ^{1}H spectrum. ROESY correlations were observed using a mixing time of 600 ms. HMBC correlations are from the proton(s) stated to the indicated ^{13}C atom.

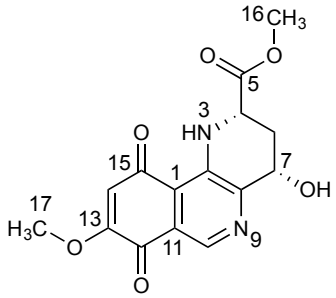

No.	δ_c	Proton	δH (J_{HH}[Hz])	HMBC[a]	ROESY
1	112.56				
2	138.34				
3		3-NH	9.22 ($J_{3,4}$ = 3.8)	1,2,4,6,8	4
4	49.12	4-H	4.49 ($J_{4,3}$ = 3.8, $J_{4,6a}$ = 6.3) ($J_{4,6b}$ = 12.2)	2,5,6,7,8	3, 6a, 6b, 7
5	172.07				
6	30.13	6-Ha	2.24 ($J_{6a,4}$ =6.3, $J_{6a,6b}$ = 13.5, $J_{6a,7}$ = 3.6)	4,5,7,8	4, 6b, 7
		6-Hb	2.38 ($J_{6b,4}$ =12.2, $J_{6a,6b}$ = 13.5) ($J_{6b,7}$ = 9.0)	4,5,7,8	4, 6a, 7
7	65.09	7-H	4.69 ($J_{7,6a}$ = 3.6, $J_{7,6b}$ = 9.0)		4, 6a, 6b, 7OH
7		7-OH	5.61 ($J_{7OH,7}$ = 4.2)	2,4,8	7
8	153.51				
9					
10	132.52	10-H	8.31	1,2w,8,11,12,13,15	
11	123.43				
12	179.63				
13	159.07				
14	111.20	14-H	6.32	1,2,12,13,15	17
15	187.38				
16	51.58	16-H3	3.63	5	4
17	56.24	17-H3	3.86	13,14	14

[a]w: weak correlation (less than ~10% of the intensity of strongest signal)

Dimethyl-**3,** ^{1}H NMR spectrum,
DMSO-d_6, 800 MHz

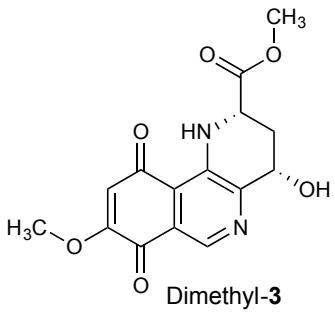

Dimethyl-**3**

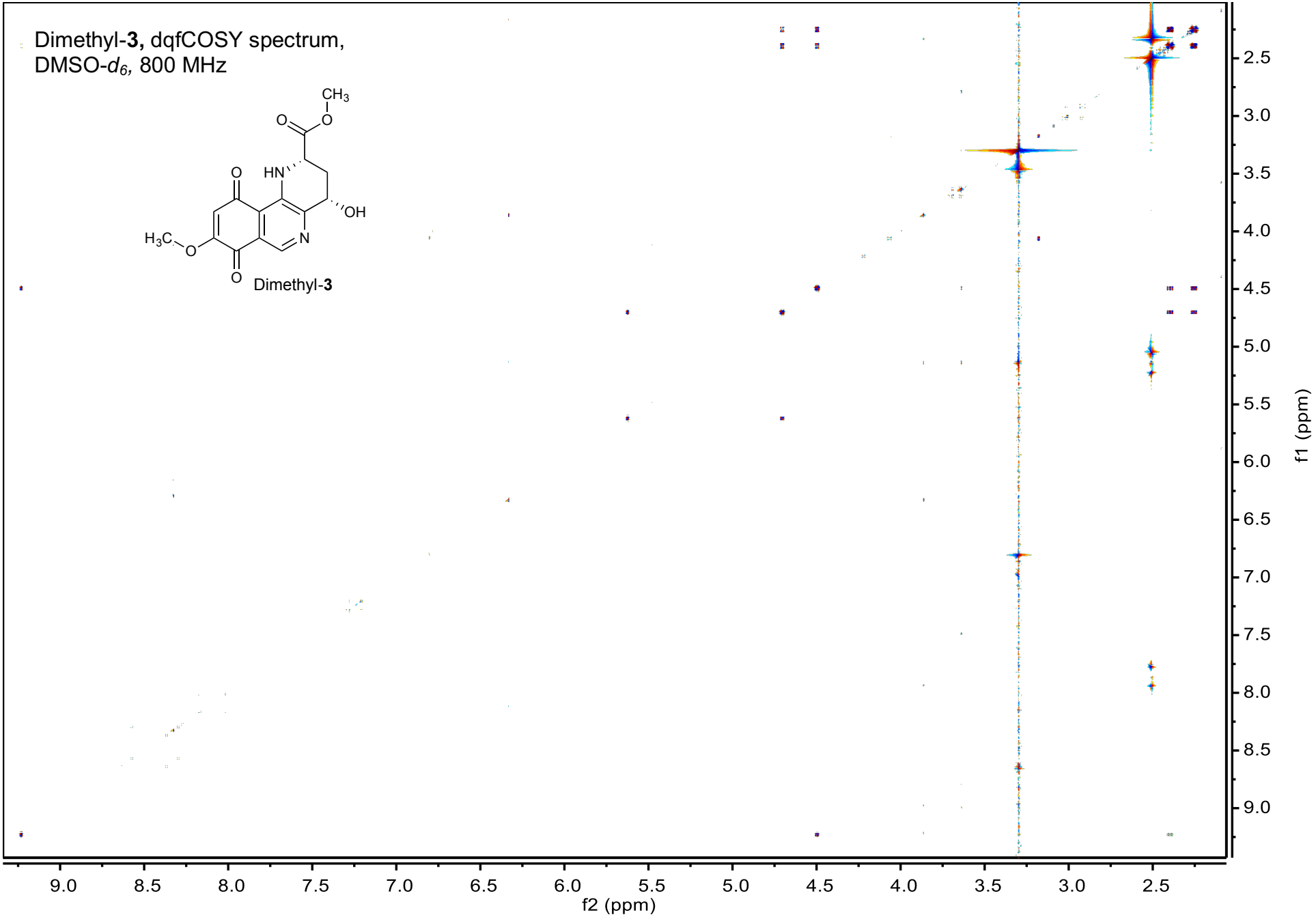
Dimethyl-3, dqfCOSY spectrum,
DMSO-d6, 800 MHz
CH3
O
O
HN
O
OH
H3C
O
N
O
Dimethyl-3
f2 (ppm)
f1 (ppm)
9.0
8.5
8.0
7.5
7.0
6.5
6.0
5.5
5.0
4.5
4.0
3.5
3.0
2.5

Dimethyl-**3,** coupled HSQC spectrum,
DMSO-d_6, 800 MHz

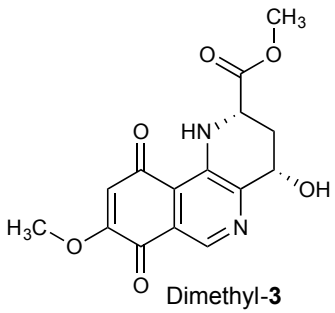

Dimethyl-**3**

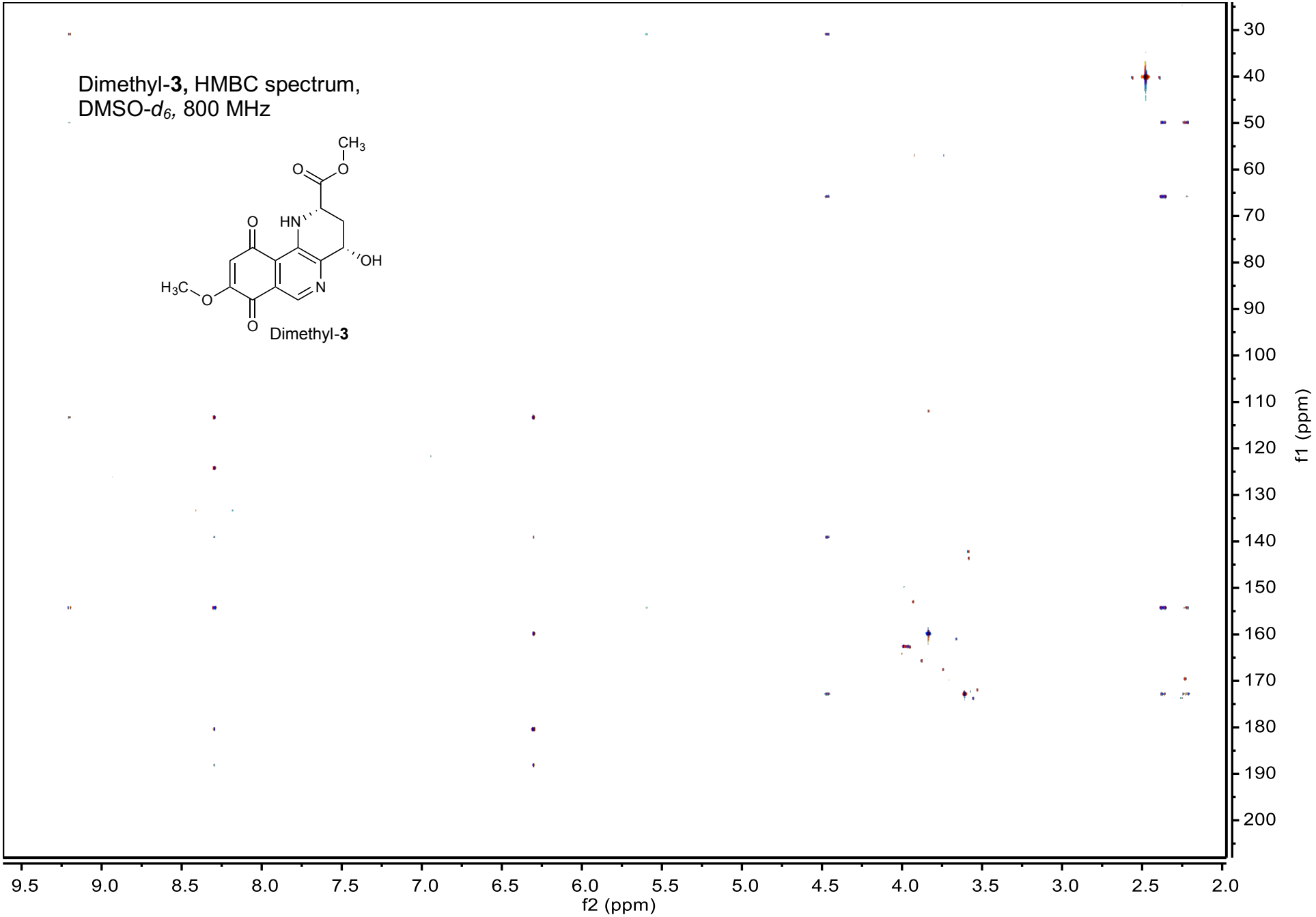
Dimethyl-3, HMBC spectrum,
DMSO-d6, 800 MHz
CH3
O
O
HN
O
OH
H3C
O
N
O
Dimethyl-3
f1 (ppm)
f2 (ppm)
9.5
9.0
8.5
8.0
7.5
7.0
6.5
6.0
5.5
5.0
4.5
4.0
3.5
3.0
2.5
2.0
30
40
50
60
70
80
90
100
110
120
130
140
150
160
170
180
190
200

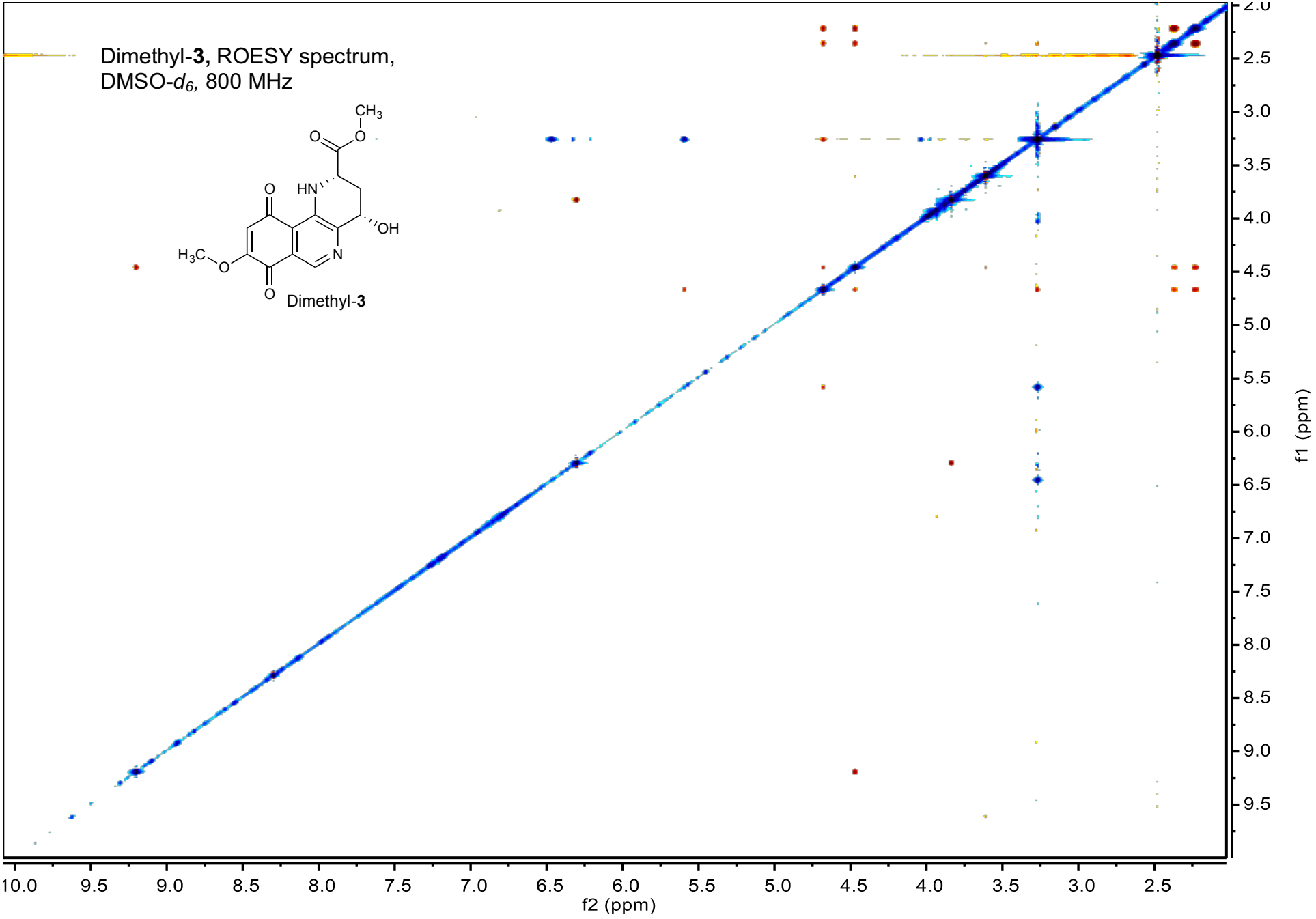
Dimethyl-3, ROESY spectrum,
DMSO-d6, 800 MHz
CH3
O
O
HN
O
OH
H3C
O
N
O
Dimethyl-3
f2 (ppm)
f1 (ppm)

^{1}H (800 MHz) and ^{13}C (200 MHz) NMR spectroscopic data for compound 4 in DMSO-d_6.

Chemical shifts were referenced to δ($C\underline{H}D_2SOCD_3$) = 2.50 and δ($^{13}\underline{C}HD_2SOCD_3$) = 39.52. ^{13}C chemical shifts were determined via HMBC and HSQC spectra. ^{1}H, ^{1}H-*J*-coupling constants were determined from the acquired ^{1}H spectrum. HMBC correlations are from the proton(s) stated to the indicated ^{13}C atom.

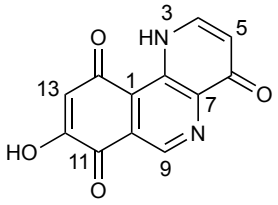

No.	δ_c	Proton	δH (J_{HH}[Hz])	HMBC[a]
1	127.41			
2	134.33			
3		3-NH	13.71 ($J_{3,4}$ = 6.6, $J_{3,5}$ = 1.7)	
4	140.30	4-H	8.06 ($J_{4,3}$ = 6.6, $J_{4,5}$ = 7.3)	2, 5, 6
5	111.88	5-H	6.24 ($J_{5,4}$ = 7.3, $J_{5,3}$ = 1.7)	4, 7
6	175.28			
7	144.61			
8				
9	141.85	9-H	8.91	1, 2w, 7, 10, 11w, 12w
10	125.00			
11	185.04			
12	180.67			
13[b]	108.10	13-H	5.45	1, 2w, 11, 12w, 14w
14[b]	172.04			

[a]w: weak correlation (less than ~10% of the intensity of strongest signals); [b]Position 12 and 14 carbon chemical shifts are interchangeable

Compound **4,** ^{1}H NMR spectrum,
DMSO-d_6, 800 MHz

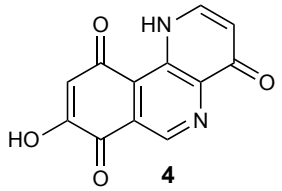

4

Compound **4,** dqfCOSY spectrum,
DMSO-d_6, 800 MHz

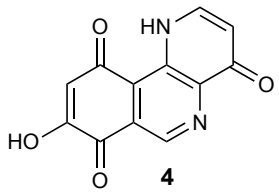

4

Compound **4,** coupled HSQC spectrum,
DMSO-d_6, 800 MHz

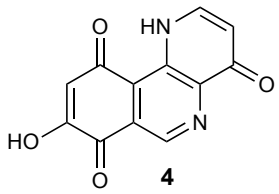

4

Compound **4,** HMBC spectrum,
DMSO-d_6, 800 MHz

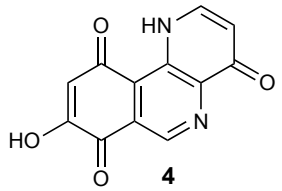

4

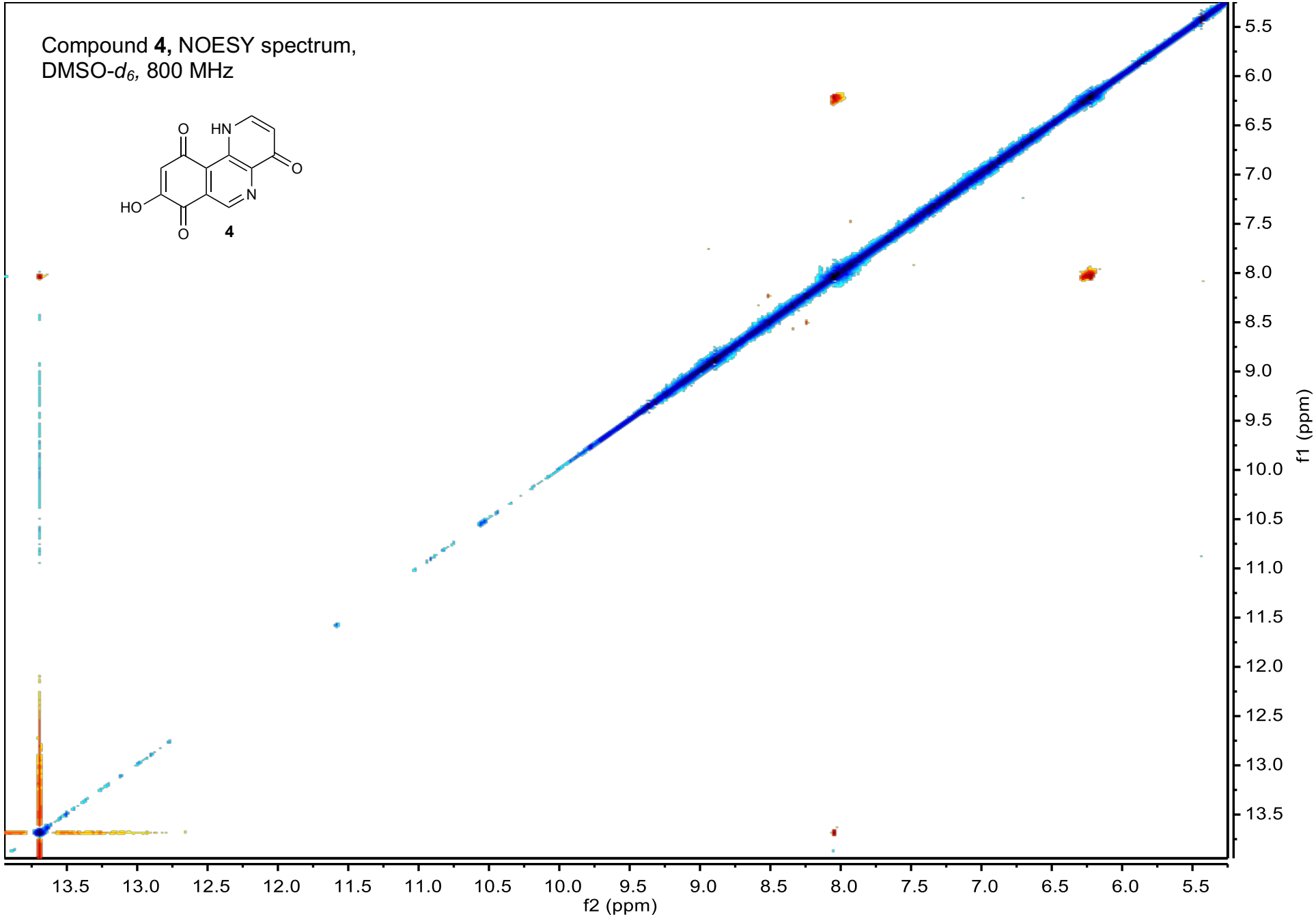
Compound 4, NOESY spectrum,
DMSO-d6, 800 MHz
O
HN
O
HO
N
O
4
5.5
6.0
6.5
7.0
7.5
8.0
8.5
9.0
9.5
10.0
10.5
11.0
11.5
12.0
12.5
13.0
13.5
f1 (ppm)
13.5
13.0
12.5
12.0
11.5
11.0
10.5
10.0
9.5
9.0
8.5
8.0
7.5
7.0
6.5
6.0
5.5
f2 (ppm)

^{1}H (800 MHz) and or ^{13}C (200 MHz) NMR spectroscopic data for compound 5 in DMSO-d_6.

Chemical shifts were referenced to δ($C\underline{H}D_2SOCD_3$) = 2.50 and δ($^{13}\underline{C}HD_2SOCD_3$) = 39.52. ^{13}C chemical shifts were determined via HMBC and HSQC spectra. ^{1}H, ^{1}H-*J*-coupling constants were determined from the acquired ^{1}H spectrum. NOESY correlations were observed using a mixing time of 600 ms. HMBC correlations are from the proton(s) stated to the indicated ^{13}C atom.

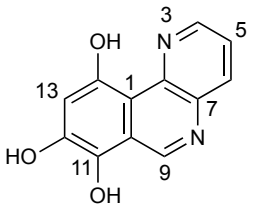

No.	δ_c	Proton	δH (J_{HH}[Hz])	HMBC[a]	NOESY
1	108.19				
2	142.74				
3					
4	146.12	4-H	8.87 ($J_{4,5}$ = 4.7)	2, 5, 6	5, 14-OH
5	121.77	5-H	7.75 ($J_{5,4}$ = 4.7, $J_{5,6}$ = 8.3)	4, 7	4, 6
6	136.97	6-H	8.48 ($J_{6,5}$ = 8.3)	2, 4	5
7	136.52				
8					
9	149.94	9-H	9.52	1, 2w, 7, 10, 11, 14w	
10	118.41				
11	133.63				
12	146.74				
13	106.91	13-H	6.97	1, 2w, 11, 12, 14	
14	150.40				
14		14-OH	13.42	1, 12, 13, 14	4

[a]w: weak correlation (less than ~10% of the intensity of strongest signal)

Compound **5,** ^{1}H NMR spectrum,
DMSO-d_6, 800 MHz

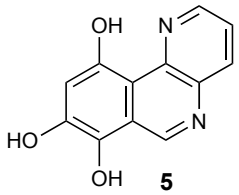

5

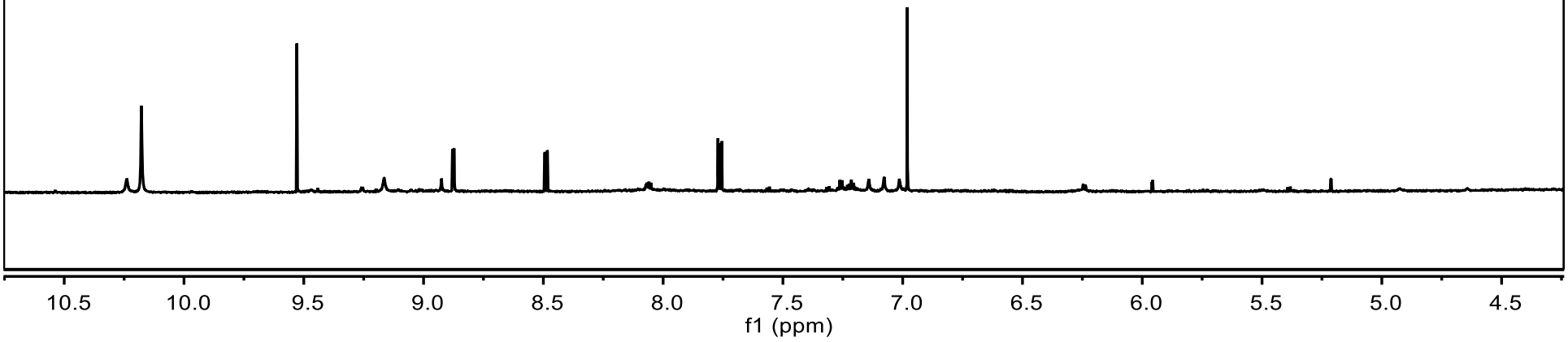

Compound **5,** dqfCOSY spectrum,
DMSO-d_6, 800 MHz

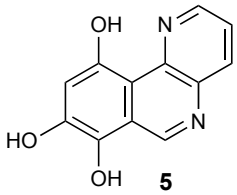

5

Compound **5,** coupled HSQC spectrum,
DMSO-d_6, 800 MHz

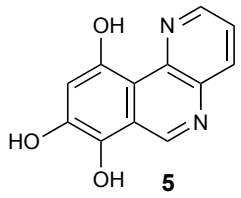

5

Compound **5,** HMBC spectrum,
DMSO-*d*$_6$, 800 MHz

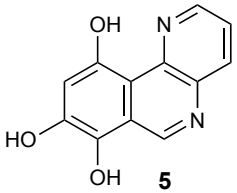

5

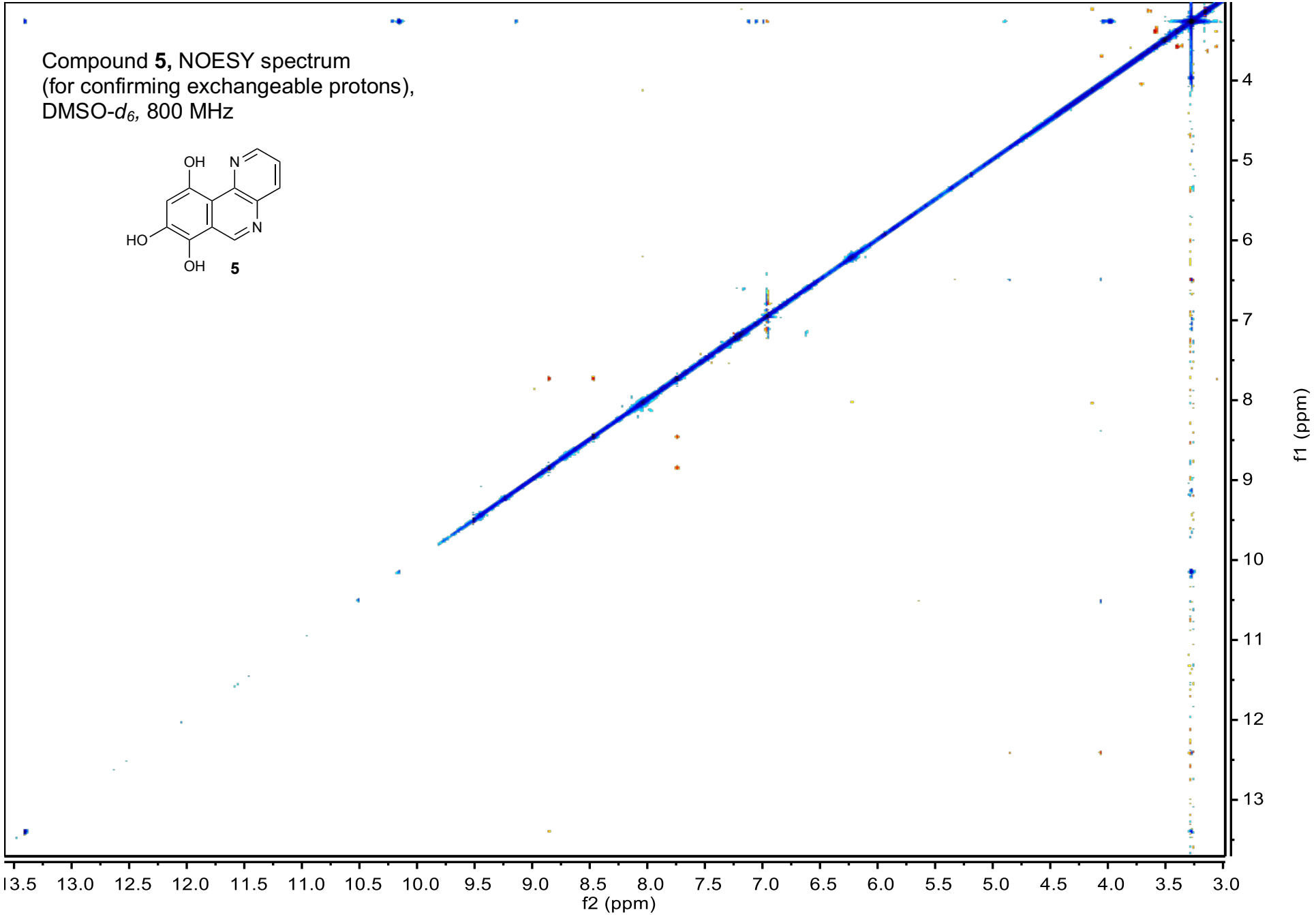
Compound 5, NOESY spectrum
(for confirming exchangeable protons),
DMSO-d6, 800 MHz
OH
N
HO
N
OH
5
f1 (ppm)
f2 (ppm)

^{1}H (600 MHz) and ^{13}C (151 MHz) NMR spectroscopic data for compound 8 in methanol-d_4.

Chemical shifts were referenced to δ(C<u>H</u>D$_2$OD) = 3.31 and δ(^{13}<u>C</u>HD$_2$OD) = 49.0. ^{13}C chemical shifts were determined via an HMBC spectrum. ^{1}H, ^{1}H-*J*-coupling constants were determined from the acquired ^{1}H spectrum. HMBC correlations are from the proton(s) stated to the indicated ^{13}C atom.

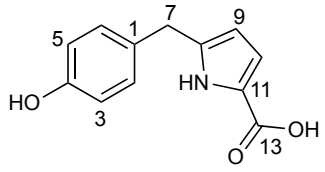

No.	δ_c	Proton	δH (J_{HH}[Hz])	HMBC
1				
2	129.62	2-H	7.03 ($J_{2,3}$ = 8.5)	1, 3, 4, 7
3	130.63	3-H	6.70 ($J_{3,2}$ = 8.5)	1, 4, 5
4	155.91			
5	130.63	5-H	6.70 ($J_{5,6}$ = 8.5)	1, 4, 5
6	129.62	6-H	7.03 ($J_{6,5}$ = 8.5)	1, 3, 4, 7
7	33.04	7-H$_2$	3.83	2, 3, 5, 6, 8, 9
8	138.30			
9	108.30	9-H	5.80 ($J_{9,10}$ = 3.5)	7, 8, 10, 11, 13
10	116.12	10-H	6.62 ($J_{10,9}$ = 3.5)	8, 9, 11, 13
11	122.63			
12		12-NH		
13	164.53			

Metabolome fraction containing **8** as major component,
^{1}H NMR spectrum in methanol-d_4, 600 MHz

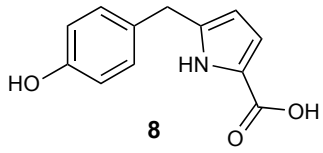

8

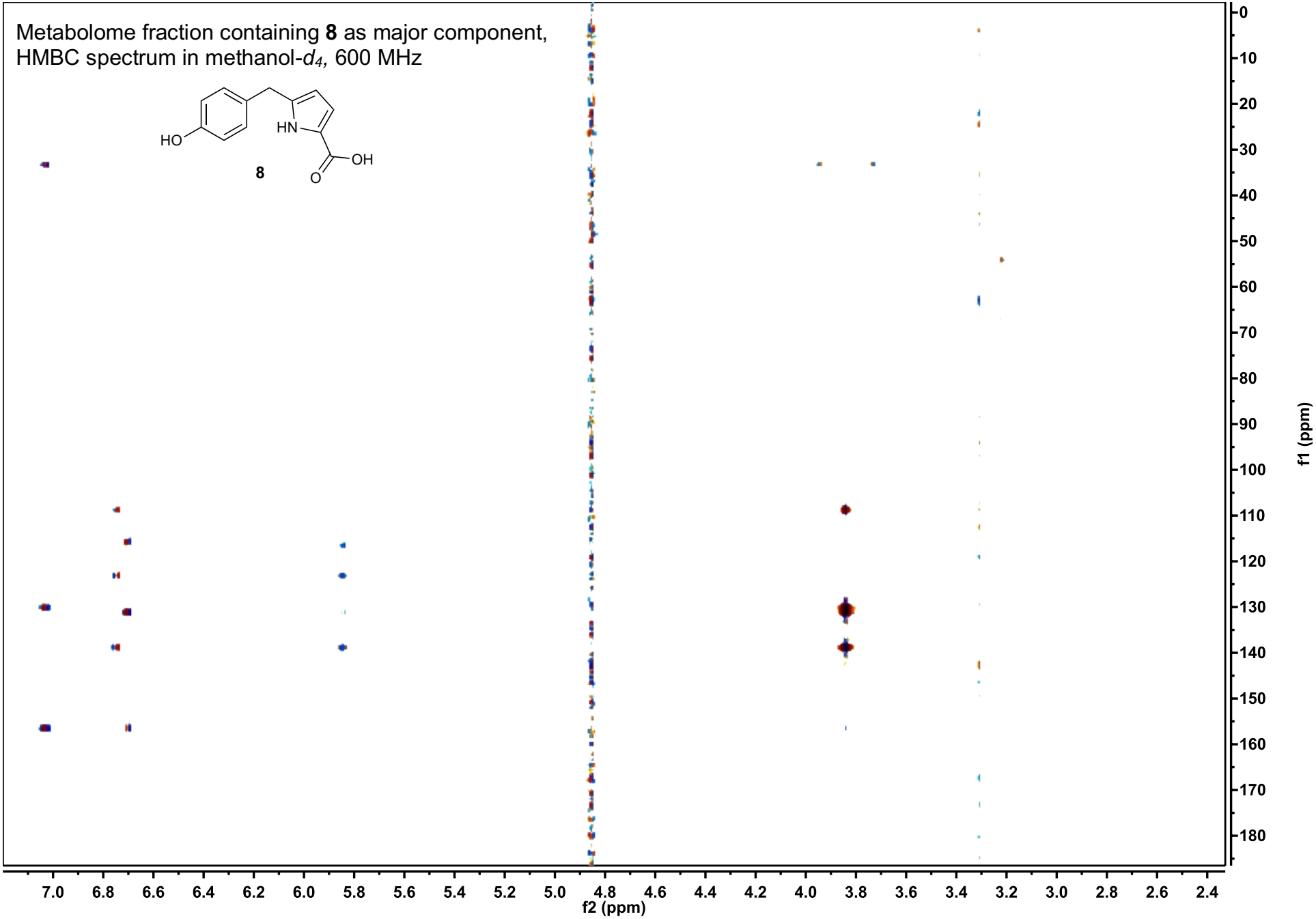
Metabolome fraction containing **8** as major component,
HMBC spectrum in methanol-d_4, 600 MHz
HO
HN
OH
O
8
f2 (ppm)
f1 (ppm)

^{1}H (500 MHz) and ^{13}C (125 MHz) NMR spectroscopic data for compound 11 in water-d_2.

Chemical shifts were referenced to δ(HOD) = 2.79 and δ(^{13}CH$_3$OD) = 49.0. ^{13}C chemical shifts were determined via an HMBC and HSQC spectrum. ^{1}H, ^{1}H-*J*-coupling constants were determined from the acquired ^{1}H spectrum. HMBC correlations are from the proton(s) stated to the indicated ^{13}C atom.

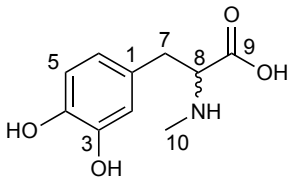

No.	δ_c	Proton	δH (J_{HH}[Hz])	HMBC
1	127.21			
2	117.10	2-H	6.84 ($J_{2,6}$ = 1.8)	4, 6, 7
3	144.36			
4	143.63			
5	116.49	5-H	6.92 ($J_{5,6}$ = 8.0)	1, 3
6	121.86	6-H	6.76 ($J_{6,5}$ = 8.0, $J_{6,2}$ = 1.8)	2, 4, 5, 7
7	35.06	7-H$_2$	3.14 ($J_{7,8}$ = 6.0)	1, 2, 6, 8, 9
8	64.71	8-H	3.82 ($J_{8,7}$ = 6.0)	1, 7, 9, 10
9	173.12			
10	32.16	10-H$_3$	2.71	8

Compound **11**, ^{1}H NMR spectrum in D_2O, 600 MHz

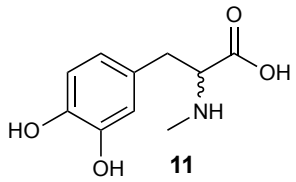

11

Compound **11**, ^{13}C NMR spectrum in D_2O, 500 MHz

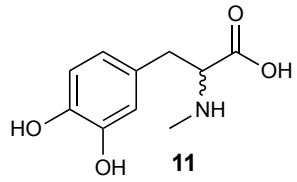

11

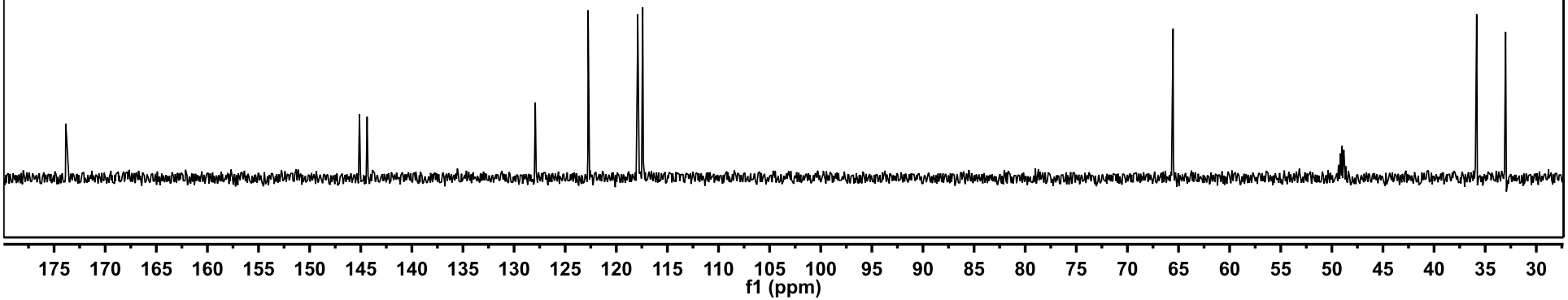

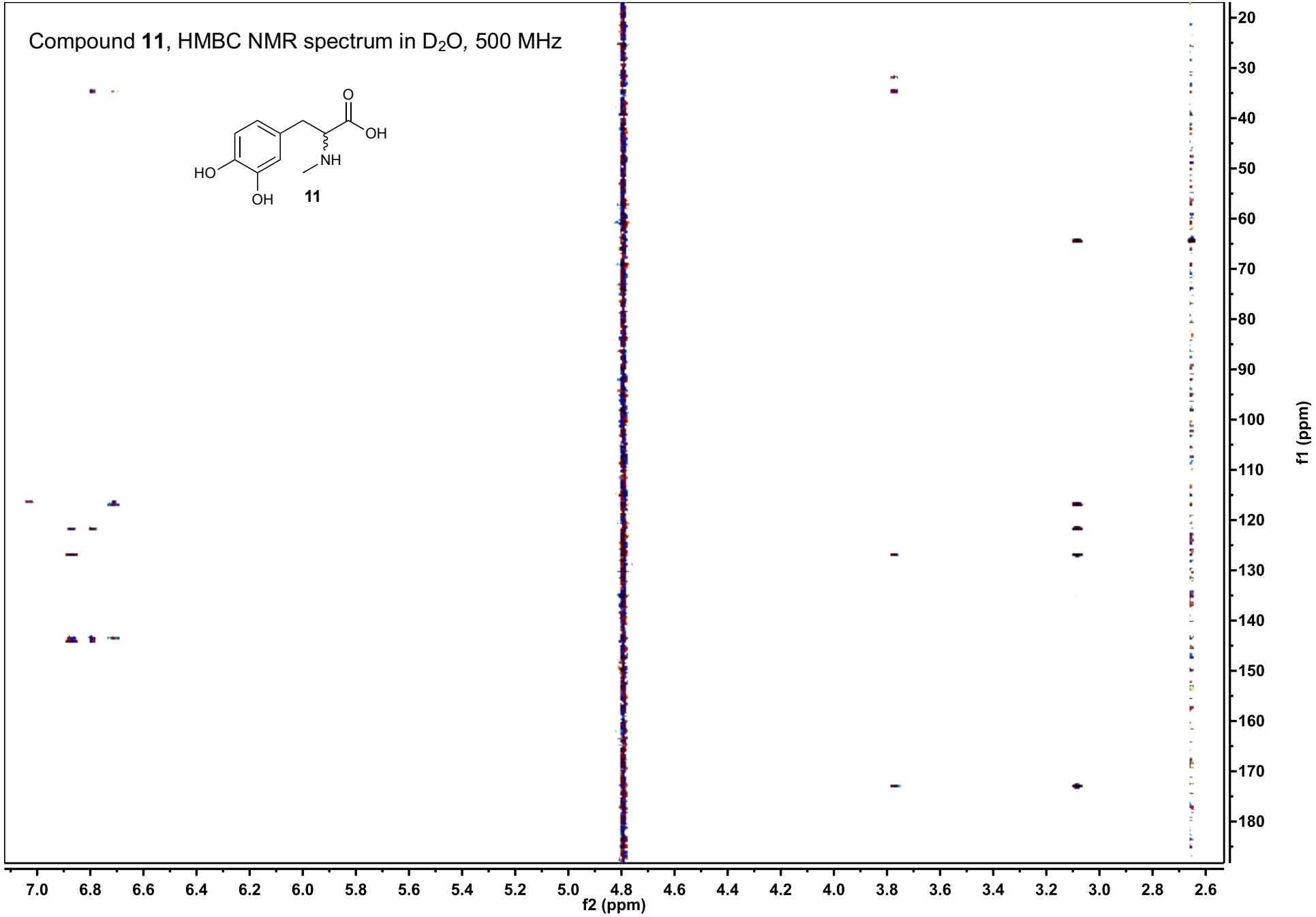
Compound **11**, HMBC NMR spectrum in D_2O, 500 MHz
HO
OH
NH
O
OH
11
f2 (ppm)
f1 (ppm)

^{1}H (600 MHz) and ^{13}C (151 MHz) NMR spectroscopic data for compound 12 in water-d_2.

Chemical shifts were referenced to δ(HOD) = 2.79 and δ(^{13}CH$_3$OD) = 49.0. ^{13}C chemical shifts were determined via an HMBC and HSQC spectrum. ^{1}H, ^{1}H-*J*-coupling constants were determined from the acquired ^{1}H spectrum. HMBC correlations are from the proton(s) stated to the indicated ^{13}C atom.

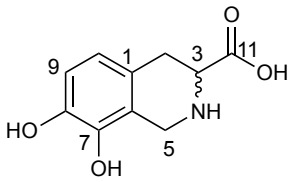

No.	δ_c	Proton	δH (J_{HH}[Hz])	HMBC
1	124.11			
2	28.50	2-Ha	3.08 ($J_{2a,2b}$ = 16.0, $J_{2a,3}$ = 11.5)	1, 3, 6, 10, 11
		2-Hb	3.32 ($J_{2b,2a}$ = 16.0, $J_{2b,3}$ = 5.0)	1, 3, 6, 10, 11
3	56.25	3-H	3.98 ($J_{3,2a}$ = 11.5, $J_{3,2b}$ = 5.0)	1, 2, 5, 11
4		4-NH		
5	40.60	5-Ha	4.25 ($J_{5a,5b}$ = 16.0)	1, 3, 6, 7
		5-Hb	4.54 ($J_{5b,5a}$ = 16.0)	1, 3, 6, 7
6	116.69			
7	140.97			
8	142.61			
9	116.49	9-H	6.93 ($J_{9,10}$ = 8.4)	1, 7
10	121.86	10-H	6.80 ($J_{10,9}$ = 8.4)	2, 6, 8
11	173.12			

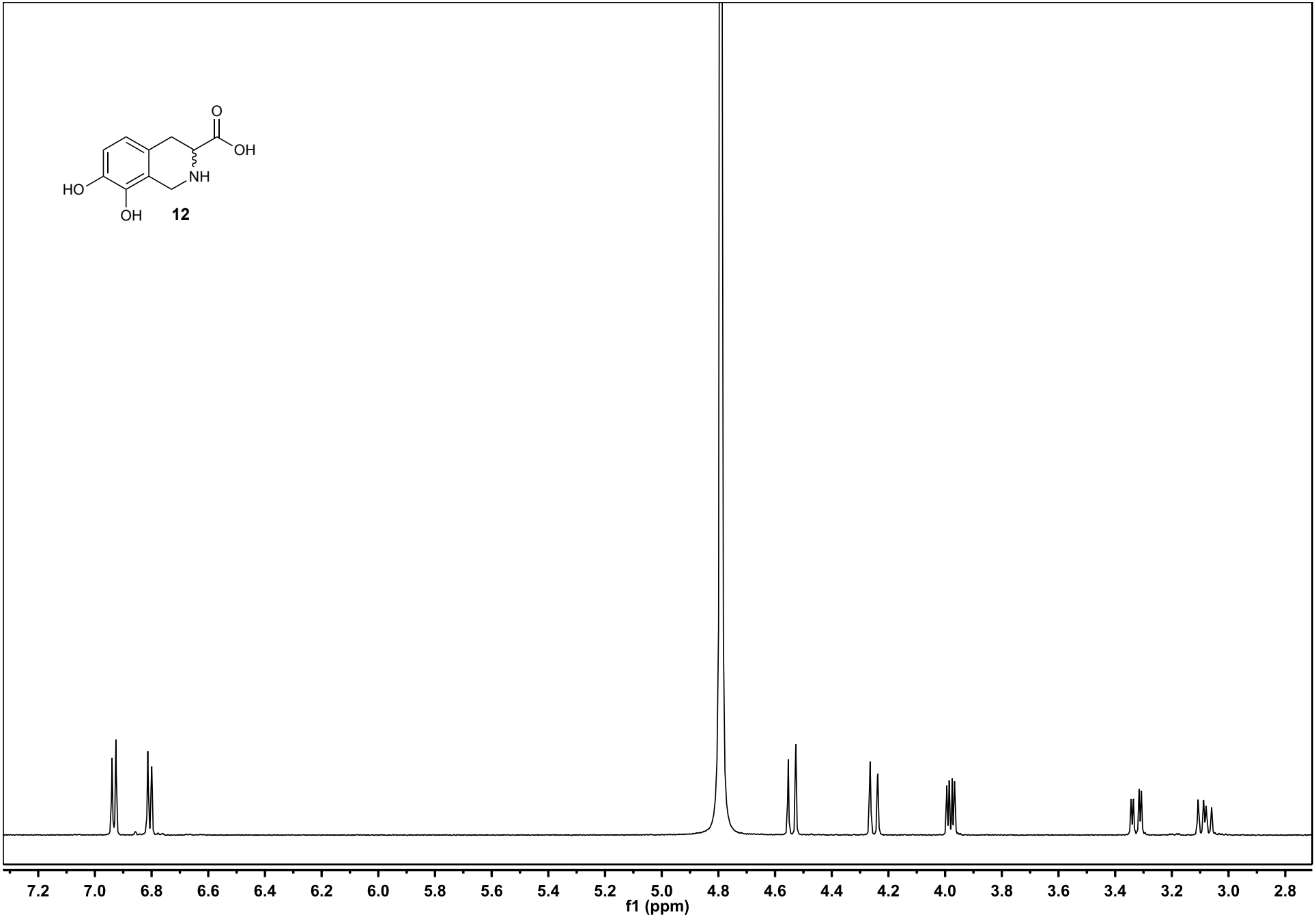
O
OH
NH
HO
OH
12
7.2
7.0
6.8
6.6
6.4
6.2
6.0
5.8
5.6
5.4
5.2
5.0
4.8
4.6
4.4
4.2
4.0
3.8
3.6
3.4
3.2
3.0
2.8
f1 (ppm)

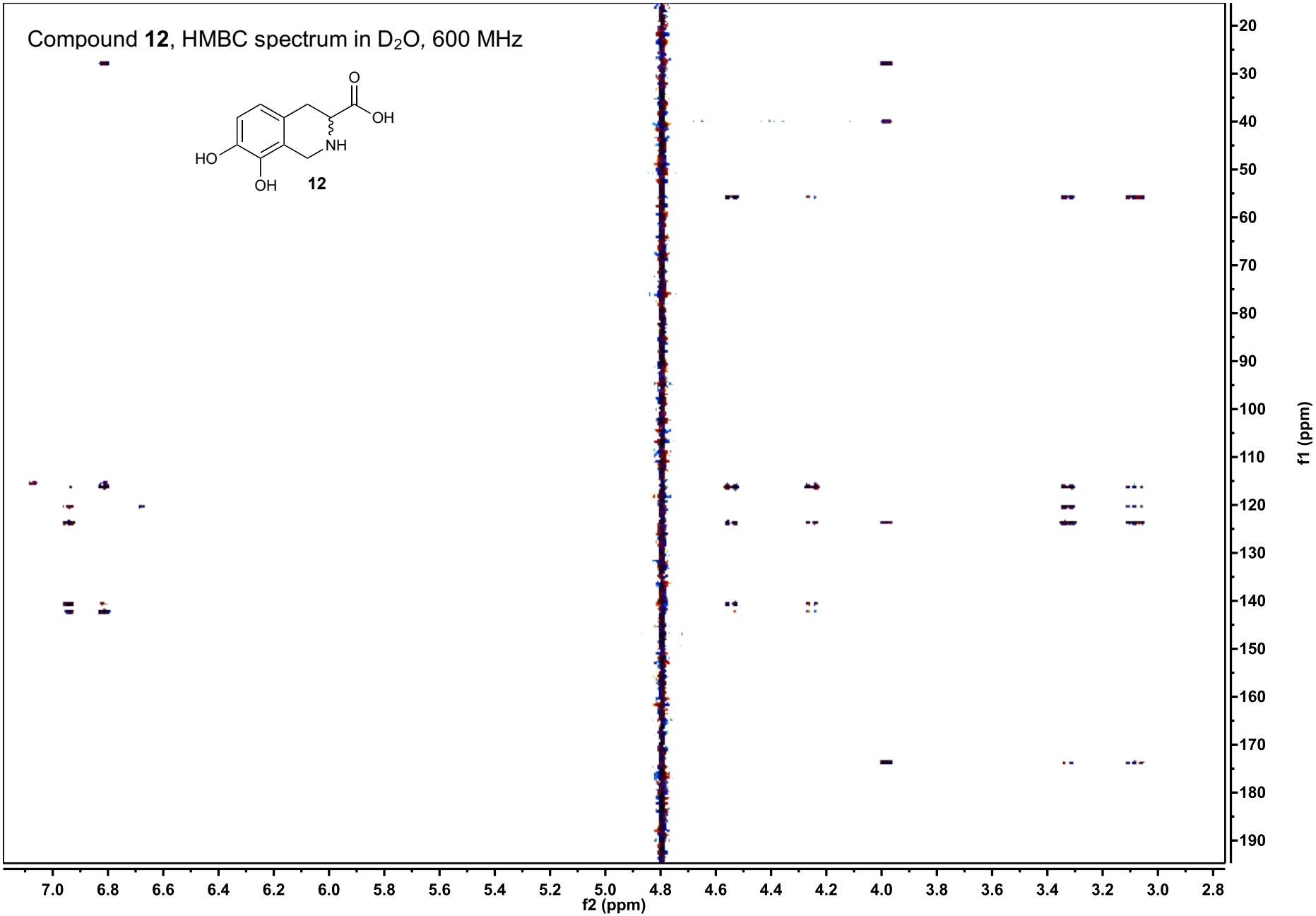
Compound 12, HMBC spectrum in D2O, 600 MHz
O
OH
NH
HO
OH
12
f2 (ppm)
f1 (ppm)

Compound **12**, decoupled HSQC spectrum in D_2O, 600 MHz

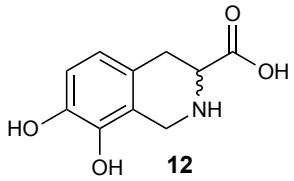

12

^{1}H (600 MHz) and ^{13}C (151 MHz) NMR spectroscopic data for compound 18 in DMSO-d_6.

Chemical shifts were referenced to δ(C<u>H</u>D$_2$SOCD$_3$) = 2.50 and δ(^{13}<u>C</u>HD$_2$SOCD$_3$) = 39.52. ^{13}C chemical shifts were determined via HMBC and HSQC spectra. ^{1}H, ^{1}H-*J*-coupling constants were determined from the acquired ^{1}H spectrum. NOESY correlations were observed using a mixing time of 600 ms. HMBC correlations are from the proton(s) stated to the indicated ^{13}C atom.

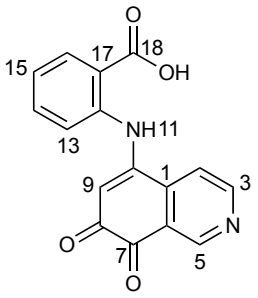

No.	δ_c	Proton	δH (J_{HH}[Hz])	HMBC[a]	NOESY
1	140.40				
2	117.23	2-H	8.05 ($J_{2,3}$ = 5.2)	3, 6, 7, 10	
3	154.59	3-H	9.02 ($J_{3,2}$ = 5.2)	1, 2, 5	
4					
5	148.00	5-H	9.08 ($J_{5,2}$ = 2.3)	1, 3, 6, 7	
6	125.13				
7	181.43				
8	175.31				
9	102.40	9-H	6.45	1, 7, 8, 10w	13
10	149.45				
11		11-NH			
12	142.36				
13	120.03	13-H	7.48 ($J_{13,14}$ = 8.5)	15, 17	9
14	130.23	14-H	7.45 ($J_{14,13}$ = 8.5, $J_{14,15}$ = 7.5)	12, 16	
15	122.68	15-H	7.11 ($J_{15,14}$ = 7.5, $J_{15,16}$ = 7.5)	13, 17	
16	131.10	16-H	8.01 ($J_{16,15}$ = 7.5)	12, 14, 18	
17	126.86				
18	168.47				

[a]w: weak correlation (less than ~10% of the intensity of strongest signal)

Metabolome fraction, containing shunt metabolite **18** as the major component, ^{1}H NMR spectrum, DMSO-d_6, 600 MHz

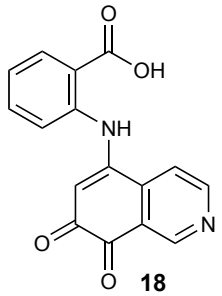

18

Metabolome fraction, containing shunt metabolite **18** as the major component, dqfCOSY spectrum, DMSO-d_6, 600 MHz

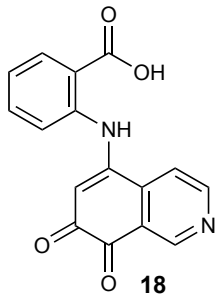

18

Metabolome fraction, containing shunt metabolite **18** as the major component, decoupled HSQC spectrum, DMSO-d_6, 600 MHz

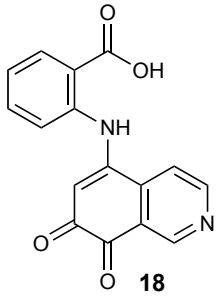

Metabolome fraction, containing shunt metabolite **18** as the major component, HMBC spectrum, DMSO-d_6, 600 MHz

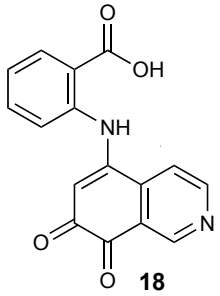

18

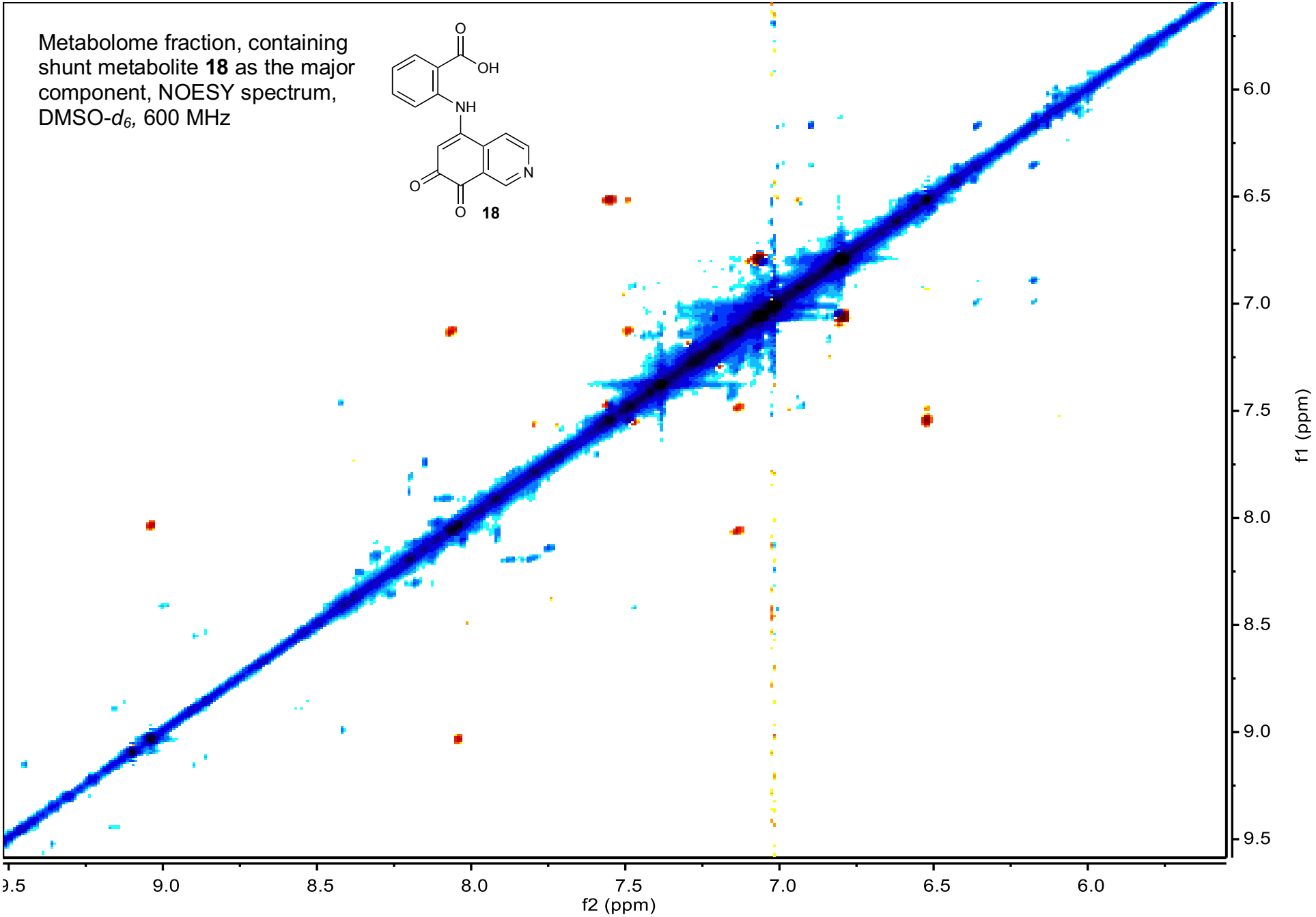
Metabolome fraction, containing shunt metabolite **18** as the major component, NOESY spectrum, DMSO-d_6, 600 MHz
O
OH
NH
N
O
O
18
6.0
6.5
7.0
7.5
8.0
8.5
9.0
9.5
f1 (ppm)
9.5
9.0
8.5
8.0
7.5
7.0
6.5
6.0
f2 (ppm)

Reaction of **11** with 0.003 equivalents of FsqB in 1 mM phosphate buffer at pH 7, ^{1}H NMR spectrum in D_2O, 600 MHz, also see Figure 5

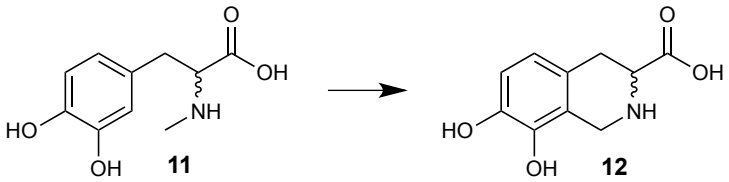

6,7-Dihydroxy-1,2,3,4-tetrahydroisoquinoline-3-carboxylic acid (**13)** in 1 mM phosphate buffer at pH 7,
^{1}H NMR spectrum water-d_2, 600 MHz

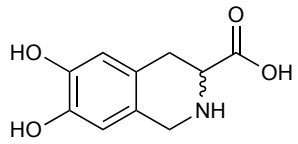

13